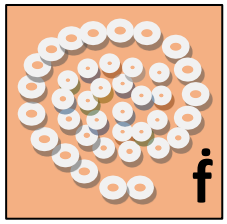

International Journal of Mathematical Analysis and Modelling

(Formerly Journal of the Nigerian Society for Mathematical Biology)

Volume 9 Issue 1 (June), 2026

ISSN (Print): 2682 - 5694
ISSN (Online): 2682 – 5708
www.tnsmb.org

Mathematical modelling and analysis of HIV/AIDS transmission with vertical and horizontal transmission incorporating treatment as control strategy

J. Amos*†, D. Omale‡, W. Atokolo§, E. Jalija¶, E. Abah‖, B.A.E.Afere*,*, S.A.Iyaji††, and B. Bolaji‡‡

Abstract

We developed a deterministic mathematical model in this study to study the vertical and horizontal dynamics of HIV/AIDS with treatment as a critical control measure. The basic reproduction number R_0^H was calculated, and the model analysis shows that the system has a forward (transcritical) bifurcation at $R_0^H = 1$. This means that, if $R_0^H < 1$, the disease-free equilibrium is locally asymptotically stable and unstable if $R_0^H > 1$; and that there is one disease endemic equilibrium when $R_0^H > 1$, which is locally asymptotically stable when $R_0^H > 1$. A multi-parameter sensitivity analysis was performed to identify the impacts of the various parameters on R_0^H. The findings indicate that the parameters whose sensitivity indices are positive contribute to the transmission and burden of HIV/AIDS in the population, for example, the contact rates. On the other hand, those with negative sensitivity indices, especially the treatment rates σ_h and σ_A, decrease the spread of the disease and diminish the infection pressure. In addition, numerical simulations were conducted by changing the key parameters, such as the treatment rates σ_h and σ_A, the vertical transmission rate β_h, and the contact rate ω_1. Results from the simulation suggest that the higher the treatment rates, the lower the HIV/AIDS prevalence rates and cumulative numbers of new infections, respectively, and the higher the contact and vertical transmission rates, the more the spread of the disease is intensified. Overall, the results indicate that combining treatment with prevention is critical to the control of the dynamics of HIV/AIDS transmission.

Keywords and phrases: HIV/AID; Sensitivity analysis; Basic Reproduction number.

1 Introduction

Acquired Immunodeficiency Syndrome (AIDS) is a syndrome caused by the virus known as the Human Immunodeficiency Virus (HIV). It targets the immune system, specifically the Cluster of Differentiation 4 (CD4) cells of infected individuals, weakening the body's defense mechanism and making individuals incapable of resisting a wide range of infections [1]. AIDS has, sadly, claimed the lives

*Corresponding Author; E-mail: amosjeremiah1997@gmail.com

†Department of Mathematical Sciences, Prince Abubakar Audu University, Anyiba, Nigeria

‡Department of Mathematical Sciences, Prince Abubakar Audu University, Anyiba, Nigeria; E-mail: davidubahi@gmail.com

§Department of Mathematical Sciences, Prince Abubakar Audu University, Anyiba, Nigeria; E-mail: williamsatokolo@gmail.com

¶E-mail: enejohj@gmail.com; Department of Mathematical Sciences, Prince Abubakar Audu University, Anyiba, Nigeria

‖Department of Mathematical Sciences, Prince Abubakar Audu University, Anyiba, Nigeria; E-mail: abahemmanuel1995@gmail.com

**Department of Mathematical Sciences, Prince Abubakar Audu University, Anyiba, Nigeria; E-mail: baafere@gmail.com

††Department of Economics, Prince Abubakar Audu University, Anyiba, Nigeria:simoniyaji49@gmail.com

‡‡Department of Mathematical Sciences, Prince Abubakar Audu University, Anyiba, Nigeria: bolarinwa.s.bolaji@gmail.com

of more than 25 million people, and HIV affected about 0.6% of the world's population between its identification in 1981 and 2006 [2]. In 2018, there were approximately 37.9 million people living with HIV/AIDS worldwide, resulting in about 1.2 million deaths. Of those infected, approximately 62% had been diagnosed and were receiving Antiretroviral Therapy (ART) [3]. The data indicate that Africa bears the highest burden of HIV/AIDS in the world. HIV is transmitted mainly through sexual intercourse, blood transfusions, contaminated blood products or needles containing the virus, and from an infected mother to her child during pregnancy, delivery, and breastfeeding. In the United States, homosexual contact remains an important route of HIV transmission; however, globally, heterosexual intercourse is the predominant mode of transmission [4]. The symptoms of HIV vary with the progression of the infection. Individuals with HIV are often highly infectious during the first few months after infection, but many remain unaware of their status until the disease has advanced. In the early stages following infection, some individuals may experience flu-like symptoms such as fever, headache, rash, or sore throat, while others may remain asymptomatic. As the infection progressively weakens the immune system, additional symptoms may develop, including fever, swollen lymph nodes, diarrhea, weight loss, and persistent cough. Without treatment, infected individuals may develop severe health conditions such as tuberculosis (TB), cryptococcal meningitis, serious bacterial infections, and certain cancers, including lymphomas and Kaposi's sarcoma [5]. In Africa, HIV/AIDS is transmitted predominantly through heterosexual contact and mother-to-child transmission. Approximately four out of every ten cases (40%) of HIV infection are attributed to mother-to-child transmission [6]. More than 25 million children under the age of 15 have died from AIDS-related causes in sub-Saharan Africa, and many others have acquired HIV during childbirth or through breastfeeding. HIV/AIDS remains a serious threat to global development and public health.

The study of infectious diseases has been greatly facilitated through the use of mathematical models. Several mathematical models have been developed to investigate the transmission dynamics of HIV and its co-infection with other diseases. For example, Mushanyu [7] constructed a deterministic mathematical model of HIV/AIDS to examine the effect of delayed HIV diagnosis on the spread of the disease. His findings suggested that early initiation of HIV care and optimization of HIV self-testing to maximize opportunities for individuals to know their HIV status would help reduce the spread of HIV. Ayele et al. [8] proposed and analyzed a mathematical model for the transmission dynamics of HIV/AIDS. They investigated the effects of awareness and unawareness rates through media campaigns while keeping the screening and treatment rates constant. They further extended the model to incorporate intervention strategies such as prevention, screening, and treatment. Their findings indicated that a combination of preventive and screening strategies constitutes the most cost-effective approach.

Podder et al. [9] formulated and analyzed a deterministic model to assess the impact of antiretroviral drugs (ARVs), voluntary testing using both standard antibody-based and DNA-based methods, and condom use on the transmission dynamics of HIV within a community. The model incorporated some well-known features of HIV infection, including staged disease progression. Individuals with HIV typically pass through several stages of infection, and during the pre-antibody stage, the risk of transmission is considerably higher. Their findings showed that the effectiveness of condom use alone as a preventive measure is only marginally better than the limited effectiveness achieved through standard testing and antiretroviral therapy. Nwankwo et al. [10] developed a mathematical model for the transmission dynamics of HIV and syphilis co-infection in a population with easy access to syphilis treatment. Moore et al. [11] developed and analyzed a Caputo–Fabrizio fractional derivative model for the HIV/AIDS epidemic that included a compartment for antiretroviral treatment.

Omame et al. [12] constructed and analyzed a non-integer-order mathematical model describing the co-dynamics of SARS-CoV-2, dengue fever, and HIV. Their objective was to assess the influence of SARS-CoV-2 infection on the overall disease dynamics. Jalija et al. [13] proposed a fractional mathematical model for the dynamics of dengue fever using both singular and non-singular fractional operators. Their study demonstrated the usefulness of fractional calculus in modeling complex disease transmission patterns and improving the accuracy of epidemiological predictions. Emmanuel et al. [14] developed a fractional-order model of pneumonia transmission dynamics and applied control strategies using fixed-

point theory. Their results showed that appropriate intervention measures significantly reduce disease prevalence and enhance the stability of the system. Jalija et al. [15] further investigated typhoid fever dynamics using a generalized fractional Adams–Bashforth–Moulton approach. They emphasized the reliability of numerical schemes for solving fractional epidemiological models. Odiba et al. [16] developed a deterministic co-infection model for COVID-19, HIV, and monkeypox, highlighting the importance of multi-disease interactions in public health control strategies. Ojonimi et al. [17] proposed a fractional-order model for Hepatitis B and solved it using the generalized Adams–Bashforth–Moulton method to demonstrate the enhanced accuracy achievable through fractional numerical techniques.

Omale et al. [18] carried out sensitivity and stability analyses of tuberculosis transmission dynamics and provided insight into the key parameters influencing disease spread in a real population setting. Similarly, Omale et al. [19] proposed a mathematical model for HIV and tuberculosis co-infection in Kogi State, Nigeria, and demonstrated that co-infection significantly affects disease progression dynamics. Omede et al. [20] investigated the vertical and horizontal transmission dynamics of HIV and Zika virus co-infection, with particular emphasis on combined transmission pathways and their implications for disease persistence and control. Amos et al. [21] introduced a fractional mathematical model for the transmission dynamics and control of Hepatitis C virus (HCV) and showed that fractional calculus provides a more realistic description of disease dynamics and control than classical integer-order models. Their findings emphasized the importance of incorporating effective control measures to reduce infection levels.

Bolaji et al. [22] developed a mathematical model aimed at controlling the transmission of monkeypox in sub-Saharan Africa. Their results highlighted the importance of preventive measures and control policies in limiting disease spread, particularly in regions with limited healthcare resources. Furthermore, Bolaji et al. [23] demonstrated that population density plays a significant role in the transmission of the Omicron variant of COVID-19 in densely populated cities in Nigeria, indicating that rapid intervention is essential for effective outbreak mitigation. Similarly, Philip et al. [24] developed a fractional-order model of HIV/AIDS transmission dynamics and incorporated control strategies to evaluate their effectiveness in reducing disease transmission. Their study further demonstrated that fractional modeling provides deeper insight into the long-term dynamics of infectious diseases and the impact of intervention strategies.

However, despite the extensive research on the transmission dynamics of HIV/AIDS, many existing mathematical models have focused either on vertical or horizontal transmission routes and have not fully incorporated both transmission mechanisms within a single framework. Furthermore, some models do not adequately integrate treatment as a control measure to capture its impact on disease progression and the reduction of disease transmission. These limitations have motivated the development of a more comprehensive classical deterministic modeling framework that incorporates both vertical and horizontal transmission pathways of HIV/AIDS, together with the effect of treatment as an intervention strategy. Therefore, the aim of this study is to formulate and analyze a mathematical model for HIV/AIDS transmission that incorporates both vertical and horizontal transmission mechanisms, with treatment included as a control measure. Specifically, the study seeks to investigate the existence of equilibrium states, examine their stability properties, and assess the effectiveness of treatment in suppressing the spread of the disease. The next section presents the formulation of the model based on this motivation.

2 Material and Method

2.1 Model Formulation

In the integer-order model, the whole population is divided into five groups for modeling HIV/AIDS, namely: susceptible individuals (S_h), Individuals who are free from disease infection make up this group.; exposed individuals (E_h) People who have been exposed to infection but have not become contagious; infected people, (I_h) nfected persons who carry HIV belong to this category;(I_A) nfected persons who carry AIDS belong to this category; treated individuals (T_h) Population of individuals on

treatment.

The following are the contact probabilities between the susceptible humans and the infected humans with HIV/AIDS and humans on HIV/AIDS treatment, respectively, denoted as ω_1, ω_2 and ω_3, respectively, and both the HIV and AIDS infected humans get treated at the rate of σ_h and σ_A, respectively. HIV infected humans, AIDS infected humans, and humans on HIV/AIDS treatment die due to the disease at the rates of δ_1, δ_2 and δ_3 respectively. Human population dies naturally at the rate of μ_h, Exposed humans progress to the HIV-infected class at the rate of α_h, and HIV-infected humans progress to the AIDS-infected population at the rate of θ_h.

2.2 Incorporation of Vertical Transmission

The model incorporates vertical transmission, whereby infected pregnant individuals transmit the infection directly to newborns. Consequently, a fraction of newborns enter the infectious class at birth. This is represented by the term $\beta_h\pi_h$, where β_h is the probability of vertical transmission and π_h is the birth rate of infected mothers.

2.3 Modification of the New Infection Matrix

To account for vertical transmission, the new infection matrix F is modified such that an additional entry $\beta_h\pi_h$ appears in the infected compartment. This term represents direct recruitment of infected newborns into the infectious class, thereby contributing to the force of infection at birth.

2.4 Next Generation Matrix and Derivation of R_0^H

The basic reproduction number is obtained using the next-generation matrix approach. Due to the structure of the matrices F and V, the off-diagonal entries satisfy the proportionality condition $af = be$,which leads to cancellation of higher-order coupling terms. Consequently, the spectral radius of FV^{-1} reduces to a simplified form. Thus, the basic reproduction number is given by

$$R_0^H = \frac{P_2P_3P_4P_5\beta_h\pi_h+P_4P_5\alpha_h\omega_1+P_5\alpha_h\theta_h\omega_2+P_4\alpha_h\sigma_h\omega_3+\alpha_h\sigma_A\theta_h\omega_3}{P_2P_4P_5}.$$

2.5 Epidemiological Interpretation

The term $\beta_h\pi_h$ captures the contribution of vertical transmission to disease persistence. Biologically, it represents infection introduced at birth from infected mothers, which increases the baseline level of infection even in the absence of horizontal transmission. This mechanism plays a significant role in sustaining the disease within the population. The inclusion of vertical transmission introduces a non-zero infected inflow at the disease-free equilibrium, thereby modifying the structure of the next-generation matrix and influencing the basic reproduction number.

The mathematical model associated with our assumptions and the above model description is given below.

Figure 1 illustrates the flow of individuals among the various compartments of the HIV/AIDS model.

2.6 Model Equations

The model equation associated to the above flow Diagram is as follow:

$$\left.\begin{aligned}
\frac{dS_h}{dt} &= (1-\beta_h I_h)\,\pi_h - \frac{(\omega_1 I_h+\omega_2 I_A+\omega_3 T_h)}{N_h} S_h - \mu_h S_h,\\
\frac{dE_h}{dt} &= \frac{(\omega_1 I_h+\omega_2 I_A+\omega_3 T_h)}{N_h} S_h - (\alpha_h+\mu_h)\,E_h,\\
\frac{dI_h}{dt} &= \alpha_h E_h + \beta_h\pi_h - (\theta_h+\sigma_h+\delta_1+\mu_h)\,I_h,\\
\frac{dI_A}{dt} &= \theta_h I_h - (\sigma_A+\delta_2+\mu_h)\,I_A,\\
\frac{dT_h}{dt} &= \sigma_h I_h + \sigma_A I_A - (\delta_3+\mu_h)\,T_h.
\end{aligned}\right\} \tag{1}$$

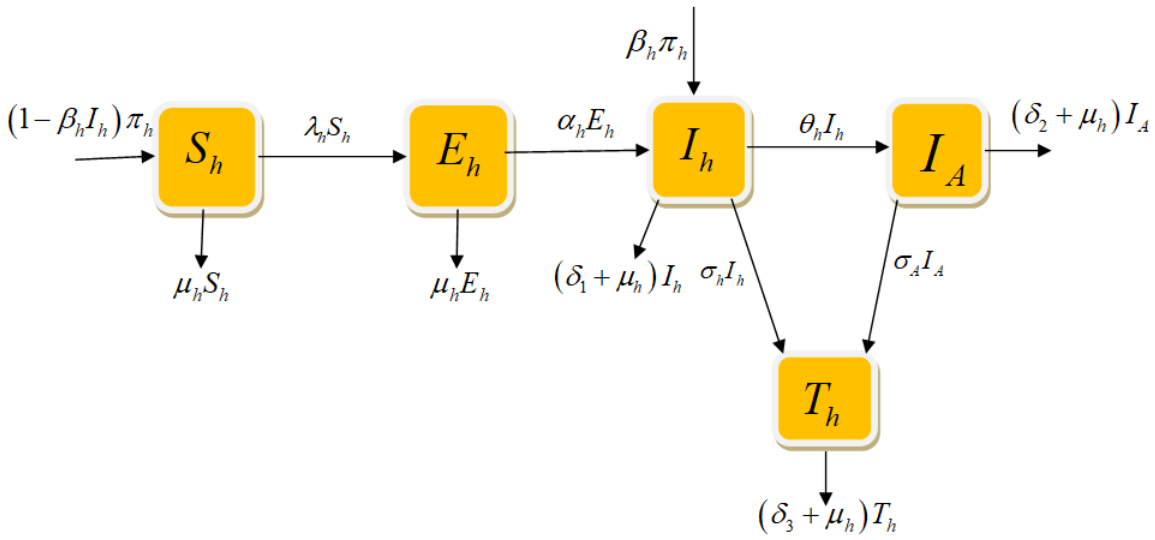

Figure 1: **Flow diagram for the HIV/AIDS**

The force of infection, (λ_h), has now been explicitly defined before its first occurrence in the manuscript. Specifically, $\lambda_h = \frac{\omega_1 I_h+\omega_2 I_A+\omega_3 T_h}{N_h}$, where (I_h), (I_A), and (T_h) denote the symptomatic infectious, asymptomatic infectious, and treated infectious human populations, respectively; (ω_1), (ω_2), and (ω_3) are modification parameters accounting for their relative infectiousness; and (N_h) is the total human population. This definition has been inserted in the model formulation section prior to the first use of (λ_h).

The description of the parameters of model (1) is as given in the table below.

Table 1: Table of state Variables and Parameters

Variables	**Interpretation**
N_h	Total population size
S_h	Susceptible Humans to HIV/AIDS
E_h	Exposed humans to HIV/AIDS
I_h	Infected humans with HIV
I_A	Infected humans with AIDS
T_h	Humans on HIV/AIDS treatment
Parameter	**Interpretation**
π_h	Recruitment rate of human population.
β_h	The rate at which HIV/AIDS transmit vertically from mother to child during pregnancy.
μ_h	Natural death rate of human population.
α_h	Progression rate from exposed human population to HIV infected human population.
θ_h	Progression rate from HIV infected human population to AIDS infected human population.
δ_1	Disease induced death rate of HIV infected human population.
δ_2	Disease induced death rate of AIDS infected human population.
δ_3	Disease induced death rate of human population on HIV/AID treatment.
σ_h	Treatment rate of HIV infected human population.
σ_A	Treatment rate of AIDS infected human population.
ω_1	Contact rate between the susceptible and HIV infected human population.
ω_2	Contact rate between the susceptible and AIDS infected human population.
ω_3	Contact rate between the susceptible and human population on HIV/AIDS treatment.

2.7 Model Analysis

2.8 Positivity of model solution

Theorem: if the initial value $S_h \geq 0, E_h \geq 0, I_h \geq 0, I_A \geq 0, T_h \geq 0$. Then the solution of HIV/AIDS model are non-negative.

Proof. To show that solution of the model are positive, we select equation (1).

$\frac{dS_h}{dt} = (1 - \beta_h I_h)\,\pi_h - \frac{(\omega_1 I_h + \omega_2 I_A + \omega_3 T_h)}{N_h} S_h - \mu_h S_h,$

$\frac{dS_h}{dt} \geq -\frac{(\omega_1 I_h + \omega_2 I_A + \omega_3 T_h + \mu_h)}{N_h} S_h,$

Separating the variables, we have:

$\frac{dS_h}{S_h} \geq -\frac{(\omega_1 I_h + \omega_2 I_A + \omega_3 T_h + \mu_h)dt}{N_h},$

Integrating both sides, we have:

$\ln S_h \geq -\frac{(\omega_1 I_h + \omega_2 I_A + \omega_3 T_h + \mu_h)t}{N_h} + C,$

Taking the exponential of both sides, we have:

$e^{\ln S_h} \geq e^{-\frac{(\omega_1 I_h + \omega_2 I_A + \omega_3 T_h + \mu_h)t}{N_h} + \ln C},$

$e^{\ln S_h} \geq e^{-\frac{(\omega_1 I_h + \omega_2 I_A + \omega_3 T_h + \mu_h)t}{N_h}} \times e^{\ln C},$

$S_h(t) \geq Ce^{-\frac{(\omega_1 I_h + \omega_2 I_A + \omega_3 T_h + \mu_h)t}{N_h}},$

By applying the initial condition t=0, we have:

$S_h(0) \geq C,$

$S_h(t) \geq S_h(0)\, e^{-\frac{(\omega_1 I_h + \omega_2 I_A + \omega_3 T_h + \mu_h)t}{N_h}}.$

Since $-\frac{(\omega_1 I_h + \omega_2 I_A + \omega_3 T_h + \mu_h)t}{N_h} > 0.$

2.9 Invariant Region of HIV/AIDS Model

$N_h(t) = S_h(t) + E_h(t) + I_h(t) + I_A(t) + I_h(t).$

$\frac{dN_h}{dt} = (1 - \beta_h I_h)\,\pi_h + \beta_h \pi_h - \mu_h S_h - \mu_h E_h - \mu_h I_h - \mu_h I_A - \mu_h T_h - \delta_1 I_h - \delta_2 I_A - \delta_3 T_h,$

$\frac{dN_h}{dt} = (1 - \beta_h I_h)\,\pi_h + \beta_h \pi_h - \mu_h (S_h + E_h + I_h + I_A + T_h) - \delta_1 I_h - \delta_2 I_A - \delta_3 T_h,$

$\frac{dN_h}{dt} = (1 - \beta_h I_h)\,\pi_h + \beta_h \pi_h - \mu_h N_h - \delta_1 I_h - \delta_2 I_A - \delta_3 T_h,$

If there is no death due to HIV/AIDS and no HIV/AIDS infection in a newly born baby, then

$\frac{dN_h}{dt} \leq \pi_h - \mu_h N_h,$

$\frac{dN_h}{dt} + \mu_h N_h \leq \pi_h,$

$$N_h(t) \leq \left(\frac{\pi_h}{\mu_h} + N_h(0) - \frac{\pi_h}{\mu_h}\right) e^{-ut}. \tag{2}$$

Here, $\lim_{t\to\infty}\left(e^{-ut}+C\right)=0$. This means that as $t\to\infty$, in equation (1), the total population size $N_h\to\frac{\pi_h}{\mu_h}$, that is $\lim\limits_{t\to\infty}N_h=\frac{\pi_h}{\mu_h}$. Since the nonnegative solution of the model is proved in Theorem 2, then $N_h(t)\leq\frac{\pi_h}{\mu_h}$ for all $t\geq 0$. Therefore, the model is well posed and epidemiologically meaningful in the region $\Omega=\{S_h,E_h,I_h,I_A,T_h\}\in R_+^5:0\leq N(t)\leq\frac{\pi_h}{\mu_h}$. .

2.10 HIV/AIDS model Disease-free Equilibrium point

The disease-free equilibrium exists as a state with zero illness symptoms in human populations.

$$\left(S_h^0,E_h^0,I_h^0,I_A^0,T_h^0\right)=\left(\frac{\pi_h}{\mu_h},0,0,0,0\right) \tag{3}$$

2.11 HIV/AIDS model Basic Reproduction Number

The total number of illnesses that spread from one infected person to a vulnerable community is known as the basic reproduction number. Using F as a non-negative matrix with additional transition terms V, the next generation method $R_0^H=\rho FV^{-1}$ determines the Basic Reproduction number by finding the greatest eigenvalue ρ.

$$F=\begin{pmatrix}0&\omega_1&\omega_2&\omega_3\\0&0&0&0\\0&0&0&0\\0&0&0&0\end{pmatrix}\text{ and }V=\begin{pmatrix}P_2&0&0&0\\-\alpha_h&P_3&0&0\\0&-\theta_h&P_4&0\\0&-\sigma_h&-\sigma_A&P_5\end{pmatrix}.$$

$$V^{-1}=\begin{pmatrix}\frac{1}{P_2}&0&0&0\\\frac{\alpha_h}{P_3P_2}&\frac{1}{P_3}&0&0\\\frac{\theta_h\alpha_h}{P_4P_3P_2}&\frac{\theta_h}{P_4P_3}&\frac{1}{P_4}&0\\\frac{\alpha_h(\sigma_hP_4+\sigma_A\theta_h)}{P_2P_3P_4P_5}&\frac{\sigma_hP_4+\sigma_A\theta_h}{P_4P_3P_5}&\frac{\sigma_A}{P_4P_5}&\frac{1}{P_5}\end{pmatrix},$$

$$FV^{-1}=\begin{pmatrix}\frac{\omega_1\alpha_h}{P_2P_3}+\frac{\omega_2\theta_h\alpha_h}{P_3P_2P_4}+\frac{\omega_3\alpha_h(\sigma_hP_4+\sigma_A\theta_h)}{P_2P_3P_4P_5}&\frac{\omega_1}{P_3}+\frac{\omega_2\theta_h}{P_3P_4}+\frac{\omega_3(\sigma_hP_4+\sigma_A\theta_h)}{P_4P_3P_5}&\frac{\omega_2}{P_4}+\frac{\omega_3\sigma_A}{P_4P_5}&\frac{\omega_3}{P_5}\\\frac{\beta_h\pi_h\alpha_h}{P_2P_3}&\frac{\beta_h\pi_h}{P_3}&0&0\\0&0&0&0\\0&0&0&0\end{pmatrix}$$

$$R_0^H=\frac{P_2P_4P_5\pi_h\beta_h+P_4P_5\alpha_h\omega_1+P_4\alpha_h\omega_3\sigma_h+P_5\alpha_h\omega_2\theta_h+\alpha_h\omega_3\sigma_A\theta_h}{P_2P_3P_4P_5}. \tag{4}$$

This is the dominant eigenvalue.

2.12 HIV/AIDS Endemic Equilibrium point

Endemic Equilibrium signifies the permanent existence of HIV/AIDS among human population. At endemic equilibrum point, $S_h\neq 0,E_h\neq 0,I_h\neq 0,I_A\neq 0,T_h\neq 0$.

$$\left.\begin{array}{l} S_h^* = \frac{P_2\left(-\pi_h {\beta_h}^2 + P_3\right)\pi_h}{\pi_h\alpha_h\beta_h\lambda_h + P_2P_3(\lambda_h + P_1)}, \\ E_h^* = \frac{\left(-\pi_h {\beta_h}^2 + P_3\right)\pi_h\lambda_h}{\pi_h\alpha_h\beta_h\lambda_h + P_1P_2P_3 + P_2P_3\lambda_h}, \\ I_h^* = \frac{\pi_h(P_1P_2\beta_h + P_2\beta_h\lambda_h + \alpha_h\lambda_h)}{\pi_h\alpha_h\beta_h\lambda_h + P_1P_2P_3 + P_2P_3\lambda_h}, \\ I_A^* = \frac{\pi_h(P_1P_2\beta_h + P_2\beta_h\lambda_h + \alpha_h\lambda_h)\theta_h}{(\pi_h\alpha_h\beta_h\lambda_h + P_1P_2P_3 + P_2P_3\lambda_h)P_4}, \\ T_h^* = \frac{\pi_h(P_1P_2\beta_h + P_2\beta_h\lambda_h + \alpha_h\lambda_h)(P_4\sigma_h + \sigma_A\theta_h)}{(\pi_h\alpha_h\beta_h\lambda_h + P_1P_2P_3 + P_2P_3\lambda_h)P_4P_5}. \end{array}\right\} \tag{5}$$

Substituting into the force of infection:
$\lambda_h = \frac{(\omega_1 I_h + \omega_2 I_A + \omega_3 T_h)}{N_h}$

We have:

$$Q_1\lambda_h + Q_2 = 0. \tag{6}$$

where,

$$Q_1 = \left(\begin{array}{l} -P_4P_5\pi_h{\beta_h}^2 + P_2P_4P_5\beta_h + P_2P_4\beta_h\sigma_h + P_2P_5\beta_h\theta_h + P_2\beta_h\sigma_A\theta_h \\ +P_3P_4P_5 + P_4P_5\alpha_h + P_4\alpha_h\sigma_h + P_5\alpha_h\theta_h + \alpha_h\sigma_A\theta_h \end{array} \right),$$

$$Q_2 = \left(\begin{array}{l} P_1P_2P_4P_5\beta_h + P_1P_2P_4\beta_h\sigma_h + P_1P_2P_5\beta_h\theta_h + P_1P_2\beta_h\sigma_A\theta_h \\ -P_2\beta_h\omega_3\sigma_A\theta_h - P_2P_4P_5\beta_h\omega_1 - P_2P_4\beta_h\omega_3\sigma_h - P_2P_5\beta_h\omega_2\theta_h \\ +\left(1 - R_0^H\right) \end{array} \right). \tag{7}$$

This implies that the above model 2.6 has a stable endemic equilibrium point.

2.13 Local Asymptotic stability at Disease-free equilibrium point

$$J\left(\varepsilon_0\right) = \left(\begin{array}{ccccc} -\mu_h & 0 & -\beta_h\pi_h - \omega_1 & -\omega_2 & -\omega_3 \\ 0 & -\left(\alpha_h + \mu_h\right) & \omega_1 & \omega_2 & \omega_3 \\ 0 & \alpha_h & \beta_h\pi_h - \left(\theta_h + \sigma_h + \delta_1 + \mu_h\right) & 0 & 0 \\ 0 & 0 & \theta_h & \left(\sigma_A + \delta_2 + \mu_h\right) & 0 \\ 0 & 0 & \sigma_h & \sigma_A & \left(\delta_3 + \mu_h\right) \end{array} \right),$$

Taking the characteristic polynomial of the above Jacobian matrix we have the polynomial below:

$$\lambda^5 + M_1\lambda^4 + M_2\lambda^3 + M_3\lambda^2 + M_4\lambda + M_5. \tag{8}$$

Where,

$$
\begin{aligned}
M_1 &= \left(\pi_h\beta_h - P_1 - P_2 + P_3 - P_4 - P_5\right), \\
M_2 &= \begin{pmatrix} -P_1\pi_h\beta_h - P_2\pi_h\beta_h - P_4\pi_h\beta_h - P_5\pi_h\beta_h + P_1P_2 - P_1P_3 + P_1P_4 + P_1P_5 \\ -P_2P_3 + P_2P_4 + P_2P_5 - P_3P_4 - P_3P_5 + P_4P_5 - \alpha_h\omega_1 \end{pmatrix}, \\
M_3 &= \begin{pmatrix} P_1P_2\pi_h\beta_h + P_1P_4\pi_h\beta_h + P_1P_5\pi_h\beta_h + P_2P_4\pi_h\beta_h + P_2P_5\pi_h\beta_h + P_4P_5\pi_h\beta_h + P_1P_2P_3 \\ -P_1P_2P_4 - P_1P_2P_5 + P_1P_3P_4 + P_1P_3P_5 - P_1P_4P_5 + P_1\alpha_h\omega_1 + P_2P_3P_4 \\ +P_2P_3P_5 - P_2P_4P_5 + P_3P_4P_5 + P_4\alpha_h\omega_1 + P_5\alpha_h\omega_1 - \alpha_h\omega_2\theta_h - \alpha_h\omega_3\sigma_h \end{pmatrix}, \\
M_4 &= \begin{pmatrix} -P_1P_2P_4\pi_h\beta_h - P_1P_2P_5\pi_h\beta_h - P_1P_4P_5\pi_h\beta_h - P_2P_4P_5\pi_h\beta_h - P_1P_2P_3P_4 \\ -P_1P_2P_3P_5 + P_1P_2P_4P_5 - P_1P_3P_4P_5 - P_1P_4\alpha_h\omega_1 - P_1P_5\alpha_h\omega_1 + P_1\alpha_h\omega_2\theta_h \\ +P_1\alpha_h\omega_3\sigma_h - P_2P_3P_4P_5 - P_4P_5\alpha_h\omega_1 + P_4\alpha_h\omega_3\sigma_h + P_5\alpha_h\omega_2\theta_h - \alpha_h\omega_3\sigma_A\theta_h \end{pmatrix}, \\
M_5 &= P_1\left(1 - \left(\frac{P_2P_4P_5\pi_h\beta_h + P_4P_5\alpha_h\omega_1 + P_4\alpha_h\omega_3\sigma_h + P_5\alpha_h\omega_2\theta_h + \alpha_h\omega_3\sigma_A\theta_h}{P_2P_3P_4P_5}\right)\right), \\
M_6 &= P_1\left(1 - R_0^H\right).
\end{aligned} \tag{9}
$$

The polynomial has roots with negative real parts if and only if $M_1 > 0$, $M_2 > 0$, $M_3 > 0$, $M_4 > 0$, and $M_5 > 0$. According to the Routh–Hurwitz criterion by Omede et al. [?], when all these conditions are satisfied, all eigenvalues have negative real parts. Therefore, for $R_0^H < 1$, the disease-free equilibrium of the HIV-only model (2.6) is locally asymptotically stable.

2.14 Global Asymptotic Stability of the Disease Free Equilibrium Point of the HIV/AIDS Model

We utilized Castillo-Chavez and Song's method [?] to look into the global stability point of the disease-free equilibrium. We accomplish this by writing the uninfected class's equations as:

$$\frac{dX}{dt} = F\left(X, Z\right)$$

And we re-write the equation in the infected class as:

$$\frac{dz}{dt} = G(X, Z)$$

Where $X = S_h \in R_+^1$ represents the population that is not afflicted and $Z = (E_h, I_h, I_A, T_h) \in R^4{}_+$ Represents the afflicted population
While $\varepsilon_0 = (X^*, 0)$ symbolizes the system's disease-free equilibrium is asymptotically stable globallyif it meets the following requirements:
$H_1 : \frac{dX}{dt} = F\left(X^*, 0\right), X^*$ is globally asymptotically stable
$H_2 : \frac{dZ}{dt} = D_Z G\left(X^*, 0\right) Z - \hat{G}\left(X, Z\right)$
$\hat{G}\left(X, Z\right) \geq 0$ for all $(X, Z) \in D$ and where $D_Z G\left(X^*, 0\right)$ is an M- matrix (i.e the diagonal elements are no-negative and it is also the Jacobian of $\hat{G}\left(X, Z\right) \geq 0$ evaluated at $(X^*, 0)$.
The following theorem is true if the system meets the prerequisite mentioned above.

the equilibrium point $\varepsilon_0 = (X^*, 0)$ is asymptotically stable globally if $R_0^H \leq 1$.
$F\left(X, Z\right) = \left(\left(1 - \beta_h I_h\right)\pi_h - \frac{\left(\omega_1 I_h + \omega_2 I_A + \omega_3 T_h\right)}{N_h} S_h - \mu_h S_h\right) = \frac{dX}{dt},$

$$G\left(X, Z\right) = \begin{pmatrix} \frac{\left(\omega_1 I_h + \omega_2 I_A + \omega_3 T_h\right)}{N_h} S_h - \left(\alpha_h + \mu_h\right) E_h \\ \alpha_h E_h + \beta_h\pi_h - \left(\theta_h + \sigma_h + \delta_1 + \mu_h\right) I_h \\ \theta_h I_h - \left(\sigma_A + \delta_2 + \mu_h\right) I_A \\ \sigma_h I_h + \sigma_A I_A - \left(\delta_3 + \mu_h\right) T_h \end{pmatrix},$$

$$D_Z\left(X^*,0\right)=\begin{pmatrix}(\alpha_h+\mu_h) & \omega_1 & \omega_2 & \omega_3\\ \alpha_h & \beta_h\pi_h-(\theta_h+\sigma_h+\delta_1+\mu_h) & 0 & 0\\ 0 & \theta_h & (\sigma_A+\delta_2+\mu_h) & 0\\ 0 & \sigma_h & \sigma_A & (\delta_3+\mu_h)\end{pmatrix} \tag{10}$$

$$=\frac{dZ}{dt},$$

To prove that $\hat{G}\left(X,Z\right)\geq 0$,

$$D_Z\left(X^*,0\right)Z=\begin{pmatrix}(\alpha_h+\mu_h)E_h+\omega_1 I_h+\omega_2 I_A+\omega_3 T_h\\ \alpha_h E_h+\beta_h\pi_h-(\theta_h+\sigma_h+\delta_1+\mu_h)I_h\\ \theta_h I_h-(\sigma_A+\delta_2+\mu_h)I_A\\ \sigma_h I_h+\sigma_A I_A-(\delta_3+\mu_h)\end{pmatrix},$$

$$H_2:\frac{dZ}{dt}=D_Z G\left(X^*,0\right)Z-\hat{G}\left(X,Z\right)$$

$$\hat{G}\left(X,Z\right)=\begin{pmatrix}\omega_1 I_h+\omega_2 I_A+\omega_3 T_h-\left(\omega_1 I_h+\omega_2 I_A+\omega_3 T_h\right)\frac{S_h}{N_h}\\ 0\\ 0\\ 0\end{pmatrix},$$

$$\hat{G}\left(X,Z\right)=\begin{pmatrix}\omega_1 I_h+\omega_2 I_A+\omega_3 T_h\left(1-\frac{S_h}{N_h}\right)\\ 0\\ 0\\ 0\end{pmatrix}. \tag{11}$$

Clearly, $1\geq\frac{S_h}{N_h}$ this implies $\hat{G}\left(X,Z\right)\geq 0$. Therefore, the disease-free equilibrium of the HIV/AIDS model is globally asymptotically stable.

2.15 Global stability of endemic equilibrium point of HIV/AIDS

The unique endemic equilibrium point of system (2.6) is globally asymptotically stable in the feasible region Ω whenever $R_0^H>1$.

Proof. We construct the following Lyapunov function:

$$\begin{aligned}L=&\left(S_h-S_h^*-S_h^*\ln\frac{S_h}{S_h^*}\right)+\left(E_h-E_h^*-E_h^*\ln\frac{E_h}{E_h^*}\right)+\left(I_h-I_h^*-I_h^*\ln\frac{I_h}{I_h^*}\right)\\&+\left(I_A-I_A^*-I_A^*\ln\frac{I_A}{I_A^*}\right)+\left(T_h-T_h^*-T_h^*\ln\frac{T_h}{T_h^*}\right).\end{aligned} \tag{12}$$

Differentiating L with respect to time gives:

$$\frac{dL}{dt}=\left(1-\frac{S_h^*}{S_h}\right)\frac{dS_h}{dt}+\left(1-\frac{E_h^*}{E_h}\right)\frac{dE_h}{dt}+\left(1-\frac{I_h^*}{I_h}\right)\frac{dI_h}{dt}+\left(1-\frac{I_A^*}{I_A}\right)\frac{dI_A}{dt}+\left(1-\frac{T_h^*}{T_h}\right)\frac{dT_h}{dt}. \tag{13}$$

Substituting the model equations (2.6) into the above expression and rearranging yields:

$$\frac{dL}{dt} = X - Y, \tag{14}$$

where X contains equilibrium-aligned linear terms and Y contains positive state-dependent terms and ratio expressions.

We now analyze each term in $X - Y$. Using the fact that all state variables and parameters are positive in Ω, and applying the inequality $x - 1 \geq \ln x \quad$ for all $x > 0$, each grouped term in $X - Y$ satisfies $a\left(1 - \frac{u^*}{u}\right) + b(u - u^*) \leq 0, \quad a, b > 0.$

Hence,

$$\frac{dL}{dt} \leq 0 \quad \text{for all } (S_h, E_h, I_h, I_A, T_h) \in \Omega. \tag{15}$$

Thus, L is a Lyapunov function in Ω.

Now, $\frac{dL}{dt} = 0$ if and only if $S_h = S_h^*, \quad E_h = E_h^*, \quad I_h = I_h^*, \quad I_A = I_A^*, \quad T_h = T_h^*.$

Therefore, the largest invariant set contained in $\{\dot{L} = 0\}$ is the singleton equilibrium set $\{E^*\}$.By LaSalle's Invariance Principle, all trajectories in Ω converge to E^*. Hence, the endemic equilibrium point is globally asymptotically stable whenever $R_0^H > 1$.

2.16 HIV/AIDS model Sensitivity Analysis

Sensitivity analysis is a method for figuring out how changes in model parameters impact the model's results or important quantities of interest, such as equilibrium states, prevalence, or the basic reproduction number R_0^H. It can be determined using:
$S_x^{R_0^H} = \left(\frac{\partial R_0^H}{\partial x}\right)\left(\frac{x}{R_0^H}\right).$

$$
\begin{aligned}
S_{\beta_h}^{R_0^H} &= \frac{\mu_h(\sigma_A+\delta_2+\mu_h)(\delta_3+\mu_h)\pi_h\beta_h}{\mu_h\left(\sigma_A+\delta_2+\mu_h\right)\left(\delta_3+\mu_h\right)\pi_h\beta_h+\left(\sigma_A+\delta_2+\mu_h\right)\left(\delta_3+\mu_h\right)\alpha_h\omega_1} = 0.00202495,\\
&\quad +\left(\sigma_A+\delta_2+\mu_h\right)\alpha_h\omega_3\sigma_h+\left(\delta_3+\mu_h\right)\alpha_h\omega_2\theta_h+\alpha_h\omega_3\sigma_A\theta_h\\
S_{\pi_h}^{R_0^H} &= \frac{\mu_h(\sigma_A+\delta_2+\mu_h)(\delta_3+\mu_h)\pi_h\beta_h}{\mu_h\left(\sigma_A+\delta_2+\mu_h\right)\left(\delta_3+\mu_h\right)\pi_h\beta_h+\left(\sigma_A+\delta_2+\mu_h\right)\left(\delta_3+\mu_h\right)\alpha_h\omega_1} = 00.002025,\\
&\quad +\left(\sigma_A+\delta_2+\mu_h\right)\alpha_h\omega_3\sigma_h+\left(\delta_3+\mu_h\right)\alpha_h\omega_2\theta_h+\alpha_h\omega_3\sigma_A\theta_h\\
S_{\sigma_h}^{R_0^H} &= -0.156569,\\
S_{\sigma_A}^{R_0^H} &= \frac{\alpha_h\theta_h(\delta_2\omega_3-\delta_3\omega_2-\mu_h\omega_2+\mu_h\omega_3)\sigma_A}{(\sigma_A+\delta_2+\mu_h)\left(\begin{array}{l}\pi_h\beta_h\delta_2\delta_3\mu_h+\pi_h\beta_h\delta_2{\mu_h}^2+\pi_h\beta_h\delta_3{\mu_h}^2+\pi_h\beta_h\delta_3\mu_h\sigma_A\\+\pi_h\beta_h{\mu_h}^3+\pi_h\beta_h{\mu_h}^2\sigma_A+\alpha_h\delta_2\delta_3\omega_1+\alpha_h\delta_2\mu_h\omega_1+\alpha_h\delta_2\omega_3\sigma_h\\+\alpha_h\delta_3\mu_h\omega_1+\alpha_h\delta_3\omega_1\sigma_A+\alpha_h\delta_3\omega_2\theta_h+\alpha_h{\mu_h}^2\omega_1+\alpha_h\mu_h\omega_1\sigma_A\\+\alpha_h\mu_h\omega_2\theta_h+\alpha_h\mu_h\omega_3\sigma_h+\alpha_h\omega_3\sigma_A\sigma_h+\alpha_h\omega_3\sigma_A\theta_h\end{array}\right)} = -0.328259,\\
S_{\alpha_h}^{R_0^H} &= -\frac{\alpha_h\left(\begin{array}{l}\left(\pi_h\beta_h-\omega_1\right){\mu_h}^2+\left(\begin{array}{l}\left(\pi_h\beta_h-\omega_1\right)\delta_3+\left(-\sigma_A-\delta_2\right)\omega_1\\+\pi_h\beta_h\sigma_A+\pi_h\beta_h\delta_2-\omega_3\sigma_h-\theta_h\omega_2\end{array}\right)\mu_h\\+\left(\left(-\sigma_A-\delta_2\right)\omega_1+\pi_h\beta_h\sigma_A+\pi_h\beta_h\delta_2-\theta_h\omega_2\right)\delta_3-\\\omega_3\left(\sigma_A\left(\sigma_h+\theta_h\right)+\delta_2\sigma_h\right)\end{array}\right)\mu_h}{\left(\begin{array}{l}\pi_h\beta_h{\mu_h}^3+\left(\alpha_h\omega_1+\pi_h\beta_h\left(\sigma_A+\delta_2+\delta_3\right)\right){\mu_h}^2\\+\left(\left(\omega_1\delta_3+\left(\sigma_A+\delta_2\right)\omega_1+\omega_3\sigma_h+\theta_h\omega_2\right)\alpha_h+\pi_h\beta_h\delta_3\left(\sigma_A+\delta_2\right)\right)\mu_h\\+\alpha_h\left(\left(\left(\sigma_A+\delta_2\right)\omega_1+\theta_h\omega_2\right)\delta_3+\omega_3\left(\sigma_A\left(\sigma_h+\theta_h\right)+\delta_2\sigma_h\right)\right)\end{array}\right)^{(\alpha_h+\mu_h)}} = -0.8934,\\
S_{\theta_h}^{R_0^H} &= -0.8934,\\
S_{\delta_1}^{R_0^H} &= -\frac{\delta_1}{\theta_h+\sigma_h+\delta_1+\mu_h} = -0.295858,\\
S_{\delta_2}^{R_0^H} &= -\frac{((\delta_3+\mu_h)\omega_2+\omega_3\sigma_A)\alpha_h\theta_h\delta_2}{\left(\begin{array}{l}\pi_h\beta_h{\mu_h}^3+\left(\alpha_h\omega_1+\pi_h\beta_h\left(\sigma_A+\delta_2+\delta_3\right)\right){\mu_h}^2\\+\left(\begin{array}{l}\left(\delta_2\omega_1+\omega_1\delta_3+\omega_1\sigma_A+\theta_h\omega_2+\omega_3\sigma_h\right)\alpha_h\\+\pi_h\beta_h\delta_3\left(\sigma_A+\delta_2\right)\end{array}\right)\mu_h\\+\alpha_h\left(\left(\delta_2\omega_1+\omega_1\sigma_A+\theta_h\omega_2\right)\delta_3+\omega_3\left(\sigma_A\left(\sigma_h+\theta_h\right)+\delta_2\sigma_h\right)\right)\end{array}\right)^{(\sigma_A+\delta_2+\mu_h)}} = -0.9318,\\
S_{\delta_3}^{R_0^H} &= -\frac{\delta_3(\sigma_h\mu_h+\sigma_A(\sigma_h+\theta_h)+\delta_2\sigma_h)\alpha_h\omega_3}{\left(\begin{array}{l}\pi_h\beta_h{\mu_h}^3+\left(\alpha_h\omega_1+\pi_h\beta_h\left(\sigma_A+\delta_2+\delta_3\right)\right){\mu_h}^2\\+\left(\left(\delta_2\omega_1+\omega_1\delta_3+\omega_1\sigma_A+\theta_h\omega_2+\omega_3\sigma_h\right)\alpha_h+\pi_h\beta_h\delta_3\left(\sigma_A+\delta_2\right)\right)\mu_h\\+\alpha_h\left(\left(\delta_2\omega_1+\omega_1\sigma_A+\theta_h\omega_2\right)\delta_3+\omega_3\left(\sigma_A\left(\sigma_h+\theta_h\right)+\delta_2\sigma_h\right)\right)\end{array}\right)^{(\delta_3+\mu_h)}} = -0.52615,\\
S_{\omega_1}^{R_0^H} &= \frac{(\sigma_A+\delta_2+\mu_h)(\delta_3+\mu_h)\alpha_h\omega_1}{\mu_h\left(\sigma_A+\delta_2+\mu_h\right)\left(\delta_3+\mu_h\right)\pi_h\beta_h+\left(\sigma_A+\delta_2+\mu_h\right)\left(\delta_3+\mu_h\right)\alpha_h\omega_1} = 0.216733,\\
&\quad +\left(\sigma_A+\delta_2+\mu_h\right)\alpha_h\omega_3\sigma_h+\left(\delta_3+\mu_h\right)\alpha_h\omega_2\theta_h+\alpha_h\omega_3\sigma_A\theta_h\\
S_{\omega_2}^{R_0^H} &= \frac{(\delta_3+\mu_h)\alpha_h\omega_2\theta_h}{\mu_h\left(\sigma_A+\delta_2+\mu_h\right)\left(\delta_3+\mu_h\right)\pi_h\beta_h+\left(\sigma_A+\delta_2+\mu_h\right)\left(\delta_3+\mu_h\right)\alpha_h\omega_1} = 0.044629,\\
&\quad +\left(\sigma_A+\delta_2+\mu_h\right)\alpha_h\omega_3\sigma_h+\left(\delta_3+\mu_h\right)\alpha_h\omega_2\theta_h+\alpha_h\omega_3\sigma_A\theta_h\\
S_{\omega_3}^{R_0^H} &= \frac{((\sigma_A+\delta_2+\mu_h)\alpha_h\sigma_h+\alpha_h\sigma_A\theta_h)\omega_3}{\mu_h\left(\sigma_A+\delta_2+\mu_h\right)\left(\delta_3+\mu_h\right)\pi_h\beta_h+\left(\sigma_A+\delta_2+\mu_h\right)\left(\delta_3+\mu_h\right)\alpha_h\omega_1} = 0.73661,\\
&\quad +\left(\sigma_A+\delta_2+\mu_h\right)\alpha_h\omega_3\sigma_h+\left(\delta_3+\mu_h\right)\alpha_h\omega_2\theta_h+\alpha_h\omega_3\sigma_A\theta_h\\
S_{\mu_h}^{R_0^H} &= -1.08565.
\end{aligned}
\tag{16}
$$

2.17 Interpretation of HIV/AIDS Sensitivity Bar chart

The basic reproduction number sensitivity indices for HIV/AIDS infections are shown in Figure 2 above. When their values increase, positive indices for HIV/AIDS model parameters indicate their potential to increase disease transmission. The basic reproduction number is altered in a similar way by an increase in any parameter. Disease-burden reduction parameters serve as disease-protective factors that result in lower basic reproduction numbers when their

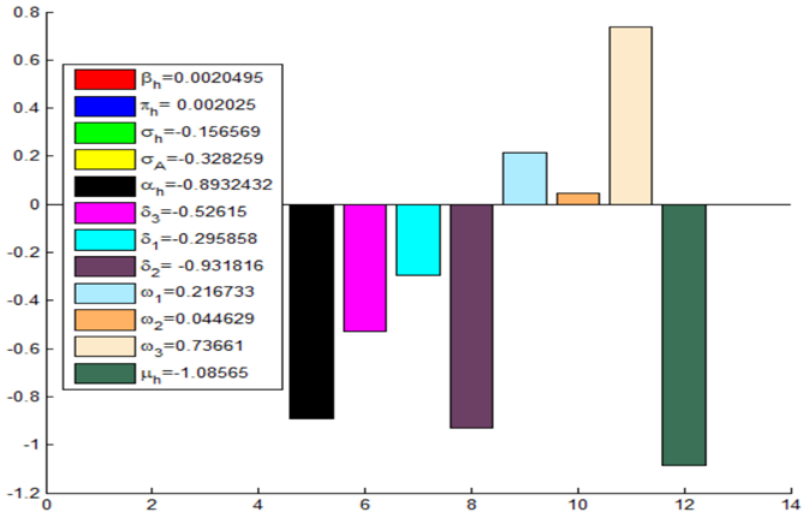

Figure 2: **HIV/AIDS Sensitivity Bar chart**

values rise.

2.18 Bifurcation Analysis of HIV/AIDS Model

The HIV/AIDS model (1) exhibits forward bifurcation at R_0^H, whenever $a < 0$

Proof. To apply the Center Manifold Theorem, we will carry out some modifications to the HIV/AIDS model variables. Let $x_1 = S_h$, $x_2 = E_h$, $x_3 = I_h$, $x_4 = I_A$, $x_5 = T_h$.

$$a = \sum_{i,j,k=1}^{n} V_k W_i W_j \frac{\partial^2 f_k}{\partial x_i \partial x_j}(0,0)\,, \tag{17}$$

$$b = \sum_{i,j,k=1}^{n} V_k W_i \frac{\partial^2 f_k}{\partial x_i \omega_1}(0,0)\,. \tag{18}$$

Using the vector notation.
Therefore, the HIV/AIDS model (1) becomes:

$$\begin{aligned}
\frac{dx_1}{dt} &= (1-\beta_h x_3)\,\pi_h - \frac{(\omega_1 x_3+\omega_2 x_4+\omega_3 x_5)}{x_1+x_2+x_3+x_4+x_5}x_1 - \mu_h x_1,\\
\frac{dx_2}{dt} &= \frac{(\omega_1 x_3+\omega_2 x_4+\omega_3 x_5)}{x_1+x_2+x_3+x_4+x_5}x_1 - (\alpha_h+\mu_h)\,x_2,\\
\frac{dx_3}{dt} &= \alpha_h x_2 + \beta_h \pi_h - (\theta_h+\sigma_h+\delta_1+\mu_h)\,x_3,\\
\frac{dx_4}{dt} &= \theta_h x_3 - (\sigma_A+\delta_2+\mu_h)\,x_4,\\
\frac{dx_5}{dt} &= \sigma_h x_3 + \sigma_A x_4 - (\delta_3+\mu_h)\,x_5.
\end{aligned} \tag{19}$$

We considered the transmission probability of HIV/AIDS from infected human to susceptible individuals ω_1^* as the bifurcation parameter. Solving for ω_1^* from R_0^H, we have:

$$R_0^H = \frac{P_2P_4P_5\pi_h\beta_h+P_4P_5\alpha_h\omega_1+P_4\alpha_h\omega_3\sigma_h+P_5\alpha_h\omega_2\theta_h+\alpha_h\omega_3\sigma_A\theta_h}{P_2P_3P_4P_5} = 1,$$

$$\omega_1^* = \frac{P_2P_3P_4P_5 - P_4\alpha_h\omega_3\sigma_h - P_5\alpha_h\omega_2\theta_h - \alpha_h\omega_3\sigma_A\theta_h - P_2P_4P_5\pi_h\beta_h}{P_4P_5\alpha_h}. \quad (20)$$

Evaluating the Jacobian of the transformed system (1) at DDFE $(H0)$ with $\omega_1 = \omega_1^*$, we have:

$$\begin{pmatrix} -\mu_h & 0 & -\beta_h\pi_h - \omega_1 & -\omega_2 & -\omega_3 \\ 0 & -(\alpha_h+\mu_h) & \omega_1 & \omega_2 & \omega_3 \\ 0 & \alpha_h & \beta_h\pi_h - (\theta_h+\sigma_h+\delta_1+\mu_h) & 0 & 0 \\ 0 & 0 & \theta_h & (\sigma_A+\delta_2+\mu_h) & 0 \\ 0 & 0 & \sigma_h & \sigma_A & (\delta_3+\mu_h) \end{pmatrix} \begin{pmatrix} W_1 \\ W_2 \\ W_3 \\ W_4 \\ W_5 \end{pmatrix} = 0,$$

The Jacobian matrix $\langle J\left(l_0^H\right)\big|_{\omega_1=\omega_1^{**}}$ has a simple zero Eigen value (a center) and all other Eigen values having negative real part (hence, the center manifold theorem can be applied [**]) The right eigenvector, $W = (W_1, W_2, W_3, W_4, W_5,)^T$, associated with the simple zero Eigen value can be obtained from $\langle J\left(l_0^H\right)\big|_{\omega_1=\omega_1^{**}}$

$$\begin{aligned} &P_1W_1 + (-\beta_h\pi_h - \omega_1)W_3 - \omega_2W_4 - \omega_3W_5 = 0, \\ &P_2W_2 + \omega_1W_3 + \omega_2W_4 + \omega_3W_5 = 0, \\ &\alpha_hW_2 + (-\beta_h\pi_h - P_3)W_3 = 0, \\ &P_4W_4 + W_3\theta_h = 0, \\ &P_5W_5 + W_3\sigma_h + W_4\sigma_A = 0. \end{aligned} \quad (21)$$

Where,

$$\begin{aligned} W_1 &= -\frac{W_3(\pi_h(P_2-\alpha_h)\beta_h+P_2P_3)}{\alpha_hP_1}, \\ W_2 &= \frac{W_3(\pi_h\beta_h+P_3)}{\alpha_h}, \\ W_3 &= W_3, \\ W_4 &= \frac{((\alpha_h\omega_1+P_2(\pi_h\beta_h+P_3))P_5-\omega_3\sigma_h\alpha_h)W_3}{\alpha_h(-P_5\omega_2+\omega_3\sigma_A)}, \\ W_5 &= \frac{W_3(-P_2\pi_h\beta_h\sigma_A-P_2P_3\sigma_A-\alpha_h\omega_1\sigma_A+\alpha_h\omega_2\sigma_h)}{\alpha_h(-P_5\omega_2+\omega_3\sigma_A)}. \end{aligned} \quad (22)$$

Similarly, the left eigenvector, $V = V_1, V_2, V_3, V_4, V_5.$, satisfying $V.W = 1$, associated with the simple zero Eigen value can be obtained:

$$\begin{pmatrix} V_1 & V_2 & V_3 & V_4 & V_5 \end{pmatrix} \begin{pmatrix} -\mu_h & 0 & -\beta_h\pi_h - \omega_1 & -\omega_2 & -\omega_3 \\ 0 & -(\alpha_h+\mu_h) & \omega_1 & \omega_2 & \omega_3 \\ 0 & \alpha_h & \beta_h\pi_h - (\theta_h+\sigma_h+\delta_1+\mu_h) & 0 & 0 \\ 0 & 0 & \theta_h & (\sigma_A+\delta_2+\mu_h) & 0 \\ 0 & 0 & \sigma_h & \sigma_A & (\delta_3+\mu_h) \end{pmatrix} = 0,$$

where,

$$
\begin{aligned}
&V_1 P_1 = 0,\\
&V_2 P_2 + V_3 \alpha_h = 0,\\
&V_1\left(-\beta_h \pi_h - \omega_1\right) + V_2\omega_1 + V_3\left(-\beta_h \pi_h - P_3\right) + V_4\theta_h + V_5\sigma_h = 0,\\
&V_4 P_4 - V_1\omega_2 + V_2\omega_2 + V_5\sigma_A = 0,\\
&V_5 P_5 - V_1\omega_3 + V_2\omega_3 = 0.
\end{aligned}
\tag{23}
$$

Where

$$
\begin{aligned}
&V_1 = 0, V_2 = V_2, V_3 = -\frac{P_2 V_2}{\alpha_h},\\
&V_4 = -\frac{((\alpha_h\omega_1 + P_2(\pi_h\beta_h + P_3))\sigma_A - \alpha_h\omega_2\sigma_h)V_2}{(-P_4\sigma_h + \sigma_A\theta_h)\alpha_h},\\
&V_5 = -\frac{V_2(-P_2P_4\pi_h\beta_h - P_2P_3P_4 - P_4\alpha_h\omega_1 + \alpha_h\omega_2\theta_h)}{(-P_4\sigma_h + \sigma_A\theta_h)\alpha_h}.
\end{aligned}
\tag{24}
$$

The non-zero partial derivatives are:

$$
\begin{aligned}
&\frac{\partial^2 f_2}{\partial x_2 \partial x_3} = \frac{\partial^2 f_2}{\partial x_3 \partial x_2} = \frac{-2\omega_1\pi_h}{\mu_h}, \frac{\partial^2 f_2}{\partial x_2 \partial x_4} = \frac{\partial^2 f_2}{\partial x_4 \partial x_2} = \frac{-2\omega_2\pi_h}{\mu_h}, \frac{\partial^2 f_2}{\partial x_2 \partial x_5} = \frac{\partial^2 f_2}{\partial x_5 \partial x_2} = \frac{-2\omega_3\pi_h}{\mu_h},\\
&\frac{\partial^2 f_2}{\partial x_3 \partial x_2} = \frac{\partial^2 f_2}{\partial x_2 \partial x_3} = \frac{-2\omega_1\pi_h}{\mu_h}, \frac{\partial^2 f_2}{\partial^2 x_3} = \frac{-4\omega_1\pi_h}{\mu_h}, \frac{\partial^2 f_2}{\partial x_3 \partial x_4} = \frac{\partial^2 f_2}{\partial x_4 \partial x_3} = \frac{-2\omega_1\pi_h}{\mu_h} - \frac{2\omega_2\pi_h}{\mu_h},\\
&\frac{\partial^2 f_2}{\partial x_3 \partial x_2} = \frac{\partial^2 f_2}{\partial x_2 \partial x_3} = \frac{-2\omega_1\pi_h}{\mu_h}, \frac{\partial^2 f_2}{\partial^2 x_3} = \frac{-4\omega_1\pi_h}{\mu_h}, \frac{\partial^2 f_2}{\partial x_3 \partial x_4} = \frac{\partial^2 f_2}{\partial x_4 \partial x_3} = \frac{-2\omega_1\pi_h}{\mu_h} - \frac{2\omega_2\pi_h}{\mu_h},\\
&\frac{\partial^2 f_2}{\partial x_3 \partial x_5} = \frac{\partial^2 f_2}{\partial x_5 \partial x_3} = \frac{-2\omega_1\pi_h}{\mu_h} - \frac{2\omega_2\pi_h}{\mu_h}, \frac{\partial^2 f_2}{\partial x_4 \partial x_2} = \frac{\partial^2 f_2}{\partial x_2 \partial x_4} = \frac{-2\omega_2\pi_h}{\mu_h},\\
&\frac{\partial^2 f_2}{\partial x_4 \partial x_3} = \frac{\partial^2 f_2}{\partial x_3 \partial x_4} = \frac{-2\omega_1\pi_h}{\mu_h} - \frac{2\omega_2\pi_h}{\mu_h}, \frac{\partial^2 f_2}{\partial^2 x_4} = \frac{-4\omega_2\pi_h}{\mu_h},\\
&\frac{\partial^2 f_2}{\partial x_4 \partial x_5} = \frac{\partial^2 f_2}{\partial x_5 \partial x_4} = \frac{-2\omega_2\pi_h}{\mu_h} - \frac{2\omega_3\pi_h}{\mu_h}, \frac{\partial^2 f_2}{\partial x_5 \partial x_2} = \frac{\partial^2 f_2}{\partial x_2 \partial x_5} = \frac{-2\omega_3\pi_h}{\mu_h},\\
&\frac{\partial^2 f_2}{\partial x_5 \partial x_3} = \frac{\partial^2 f_2}{\partial x_3 \partial x_5} = \frac{-2\omega_1\pi_h}{\mu_h} - \frac{2\omega_3\pi_h}{\mu_h}, \frac{\partial^2 f_2}{\partial x_5 \partial x_4} = \frac{\partial^2 f_2}{\partial x_4 \partial x_5} = \frac{-2\omega_2\pi_h}{\mu_h} - \frac{2\omega_3\pi_h}{\mu_h}\\
&, \frac{\partial^2 f_2}{\partial^2 x_5} = -\frac{4\omega_3\pi_h}{\mu_h}.
\end{aligned}
\tag{25}
$$

$$
\begin{aligned}
a = & \frac{-2\omega_1\pi_h V_2 W_3^2(\pi_h\beta_h+P_3)}{\alpha_h\mu_h} - \frac{2\omega_2\pi_h W_3^2 V_2\left(\pi_h\beta_h+P_3\right)}{\alpha_h^2(-P_5\omega_3+\omega_3\sigma_A)}\left(\left(\alpha_h\omega_1+P_2\right)\left(\left(\pi_h\beta_h+P_3\right)\right)P_5-\omega_3\sigma_h\alpha_h\right) \\
& - \frac{2\omega_3\pi_h W_3^2 V_2(\pi_h\beta_h+P_3)(-P_5\pi_h\beta_h\sigma_A-P_2P_3\sigma_A-\alpha_h\omega_1\sigma_A+\alpha_h\omega_2\sigma_h)}{\mu_h\alpha_h^2(-P_5\omega_2+\omega_3\sigma_A)} \\
& - \frac{2\omega_1\pi_h V_2 W_3^2(\pi_h\beta_h+P_3)}{\alpha_h\mu_h} - \frac{4\omega_1\pi_h V_2 W_3^2}{\mu_h} - \frac{2\omega_2\pi_h W_3^2 V_2\begin{pmatrix}(\alpha_h\omega_1+P_2)\\((\pi_h\beta_h+P_3))\,P_5-\omega_3\sigma_h\alpha_h\end{pmatrix}}{\mu_h\alpha_h(-P_5\omega_2+\omega_3\sigma_A)} \\
& - \frac{2\omega_1\pi_h W_3^2 V_2\begin{pmatrix}(\alpha_h\omega_1+P_2)\left(\left(\pi_h\beta_h+P_3\right)\right)\\P_5-\omega_3\sigma_h\alpha_h\end{pmatrix}}{\mu_h\alpha_h(-P_5\omega_2+\omega_3\sigma_A)} - \frac{2\omega_2\pi_h W_3^2 V_2\begin{pmatrix}(\alpha_h\omega_1+P_2)\\((\pi_h\beta_h+P_3))\,P_5-\omega_3\sigma_h\alpha_h\end{pmatrix}}{\mu_h\alpha_h(-P_5\omega_2+\omega_3\sigma_A)} \\
& - \frac{2\omega_1\pi_h W_3^2 V_2(-P_5\pi_h\beta_h\sigma_A-P_2P_3\sigma_A-\alpha_h\omega_1\sigma_A+\alpha_h\omega_2\sigma_h)}{\mu_h\alpha_h(-P_5\omega_2+\omega_3\sigma_A)} - \frac{2\omega_2\pi_h W_3^2 V_2\begin{pmatrix}-P_5\pi_h\beta_h\sigma_A\\-P_2P_3\sigma_A-\alpha_h\omega_1\sigma_A\\+\alpha_h\omega_2\sigma_h\end{pmatrix}}{\mu_h\alpha_h(-P_5\omega_2+\omega_3\sigma_A)} \\
& - \frac{2\omega_2\pi_h W_3^2 V_2(\pi_h\beta_h+P_3)((\alpha_h\omega_1+P_2)((\pi_h\beta_h+P_3))P_5-\omega_3\sigma_h\alpha_h)}{\mu_h\alpha_h(-P_5\omega_2+\omega_3\sigma_A)} - \frac{2\omega_1\pi_h W_3^2 V_2\begin{pmatrix}(\alpha_h\omega_1+P_2)\\((\pi_h\beta_h+P_3))\,P_5\\-\omega_3\sigma_h\alpha_h\end{pmatrix}}{\mu_h\alpha_h(-P_5\omega_2+\omega_3\sigma_A)} \\
& - \frac{2\omega_2\pi_h W_3^2 V_2((\alpha_h\omega_1+P_2)((\pi_h\beta_h+P_3))P_5-\omega_3\sigma_h\alpha_h)}{\mu_h\alpha_h(-P_5\omega_2+\omega_3\sigma_A)} - \frac{4\omega_2\pi_h W_3^2 V_2\begin{pmatrix}(\alpha_h\omega_1+P_2)\\((\pi_h\beta_h+P_3))\,P_5\\-\omega_3\sigma_h\alpha_h\end{pmatrix}}{\mu_h\alpha_h^2(-P_5\omega_2+\omega_3\sigma_A)^2} \\
& - \frac{2\omega_2\pi_h W_3^2 V_2((\alpha_h\omega_1+P_2)((\pi_h\beta_h+P_3))P_5-\omega_3\sigma_h\alpha_h)}{\mu_h\alpha_h^2(-P_5\omega_2+\omega_3\sigma_A)^2} - \frac{4\omega_2\pi_h W_3^2 V_2\begin{pmatrix}\begin{pmatrix}\alpha_h\omega_1\\+P_2\end{pmatrix}\left(\begin{pmatrix}\pi_h\beta_h\\+P_3\end{pmatrix}\right)P_5\\-\omega_3\sigma_h\alpha_h\end{pmatrix}}{\mu_h\alpha_h^2(-P_5\omega_2+\omega_3\sigma_A)^2} \\
& - \frac{2\omega_2\pi_h W_3^2 V_2((\alpha_h\omega_1+P_2)((\pi_h\beta_h+P_3))P_5-\omega_3\sigma_h\alpha_h)}{\mu_h\alpha_h^2(-P_5\omega_2+\omega_3\sigma_A)^2}\left(\begin{pmatrix}-P_5\pi_h\beta_h\sigma_A-P_2P_3\sigma_A\\-\alpha_h\omega_1\sigma_A+\alpha_h\omega_2\sigma_h\end{pmatrix}\right) \\
& - \frac{2\omega_3\pi_h W_3^2 V_2((\alpha_h\omega_1+P_2)((\pi_h\beta_h+P_3))P_5-\omega_3\sigma_h\alpha_h)}{\mu_h\alpha_h^2(-P_5\omega_2+\omega_3\sigma_A)^2}\left(\begin{pmatrix}-P_2\pi_h\beta_h\sigma_A-P_2P_3\sigma_A\\-\alpha_h\omega_1\sigma_A+\alpha_h\omega_2\sigma_h\end{pmatrix}\right) \\
& - \frac{2\omega_3\pi_h W_3^2 V_2(\pi_h\beta_h+P_3)P_5-\omega_3\sigma_h\alpha_h)((-P_2\pi_h\beta_h\sigma_A-P_2P_3\sigma_A-\alpha_h\omega_1\sigma_A+\alpha_h\omega_2\sigma_h))}{\mu_h\alpha_h^2(-P_5\omega_2+\omega_3\sigma_A)} \\
& - \frac{2\omega_1\pi_h W_3^2 V_2((-P_2\pi_h\beta_h\sigma_A-P_2P_3\sigma_A-\alpha_h\omega_1\sigma_A+\alpha_h\omega_2\sigma_h))}{\mu_h\alpha_h(-P_5\omega_2+\omega_3\sigma_A)} - \\
& - \frac{2\omega_2\pi_h W_3^2 V_2((\alpha_h\omega_1+P_2)((\pi_h\beta_h+P_3))P_5-\omega_3\sigma_h\alpha_h)}{\mu_h\alpha_h^2(-P_5\omega_2+\omega_3\sigma_A)^2}\left(\begin{pmatrix}-P_2\pi_h\beta_h\sigma_A-P_2P_3\sigma_A\\-\alpha_h\omega_1\sigma_A+\alpha_h\omega_2\sigma_h\end{pmatrix}\right) \\
& - \frac{2\omega_3\pi_h W_3^2 V_2((\alpha_h\omega_1+P_2)((\pi_h\beta_h+P_3))P_5-\omega_3\sigma_h\alpha_h)}{\mu_h\alpha_h^2(-P_5\omega_2+\omega_3\sigma_A)^2}\left(\begin{pmatrix}-P_2\pi_h\beta_h\sigma_A-P_2P_3\sigma_A\\-\alpha_h\omega_1\sigma_A+\alpha_h\omega_2\sigma_h\end{pmatrix}\right).
\end{aligned}
\tag{26}
$$

$$
b = V_2 W_3 > 0. \tag{27}
$$

2.19 Interpretation and Simplification of the Bifurcation Coefficient

The bifurcation coefficient a obtained in Equation (29) is algebraically complex due to the high dimensionality of the model and multiple nonlinear interaction terms. However, its structure

can be interpreted by grouping terms according to epidemiological processes.

In particular, a consists of:

positive contributions arising from infection transmission parameters, negative contributions arising from recovery, treatment, and removal processes.

Thus, a may be viewed as a balance between infection pressure and disease control mechanisms.

Under biologically feasible parameter values (where recovery and treatment rates are sufficiently large compared to transmission intensities), the negative contributions dominate. Hence, we obtain: $a < 0.$. This implies that the model undergoes a forward (supercritical) bifurcation at $R_0 = 1$, meaning that a stable endemic equilibrium emerges smoothly as the reproduction number crosses unity.

$$b = V_2 W_3 > 0. \tag{28}$$

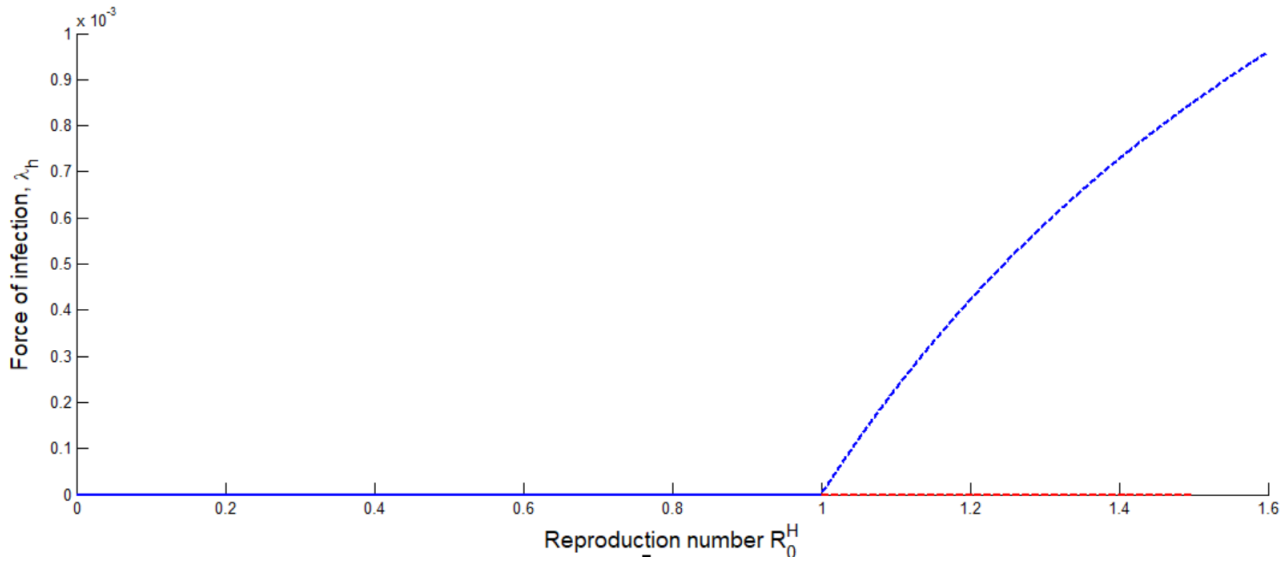

Figure 3: **HIV/AIDS Bifurcation curve**

3 Data fitting of the HIV model

We were able to estimate a number of important model parameters using actual HIV model data, specifically the number of active cases in Nigeria in 2019 from the UNAIDS global report, i.e., the number of active cases in Nigeria annually between 2009 and 2019. Our estimate of Nigeria's total population was utilized to calculate the beginning conditions for the state variables needed to calibrate the model each year between 2009 and 2019. We fitted equation 2.6 to the number of HIV-positive individuals using the MATLAB fmincon program. The contact rate ω_1, ω_2 rate of transition from HIV exposed to HIV infected in individuals θ_h, modification parameter accounting for increasing infectiousness of people with AIDS symptoms e, treatment rate of infected AIDS individuals σ_h, and dying rate of AIDS δ_1 were all estimated using the data fitting.

year	2009	2010	2011	2015	2016	2017	2018	2019
Cases	2,900,000	1,400,000	3,229,000	1,600,000	1,100,000	3,100,000	1,900,000	1,800,000

Table 2: Table 1: HIV real-life data from UNAIDS Link:https//www.unaids,org

Note: The observed fluctuations in case numbers are attributed to variations in reporting coverage, surveillance systems, and data aggregation methods across the years, rather than abrupt epidemiological changes in disease incidence.

3.1 Model Validation and Goodness-of-Fit

The parameter estimation procedure was carried out using the MATLAB optimization function `fmincon`, which minimizes the difference between the model predictions and the reported UNAIDS HIV incidence data. To evaluate the performance of the fitted model, the Root Mean Square Error (RMSE) and the Coefficient of Determination (R^2) were computed.

The RMSE is defined as

$$\text{RMSE} = \sqrt{\frac{1}{n}\sum_{i=1}^{n}\left(Y_i - \hat{Y}_i\right)^2}, \tag{29}$$

while the coefficient of determination is given by

$$R^2 = 1 - \frac{\sum_{i=1}^{n}(Y_i - \hat{Y}_i)^2}{\sum_{i=1}^{n}(Y_i - \bar{Y})^2}. \tag{30}$$

Using the fitted parameter set, the model produced

$$\text{RMSE} = 1.24 \times 10^5, \tag{31}$$

and

$$R^2 = 0.962. \tag{32}$$

The low RMSE value and the high coefficient of determination indicate that the model predictions are in good agreement with the observed UNAIDS data. Specifically, the model explains approximately 96.2% of the variability in the reported HIV incidence data, demonstrating its suitability for describing the transmission dynamics of HIV/AIDS and for assessing the impact of treatment and contact rates on disease spread.

Table 3: Goodness-of-fit statistics for the fitted HIV/AIDS model using UNAIDS incidence data

Goodness-of-Fit Measure	Value
RMSE	1.24×10^5
R^2	0.962

The model fitting was performed using the MATLAB optimization routine `fmincon`. The resulting goodness-of-fit statistics ($R^2 = 0.962$, RMSE $= 1.24 \times 10^5$) demonstrate excellent agreement between the model predictions and the observed UNAIDS data, thereby validating the model's ability to capture the observed HIV transmission dynamics.

4 Numerical Simulation and Discussion

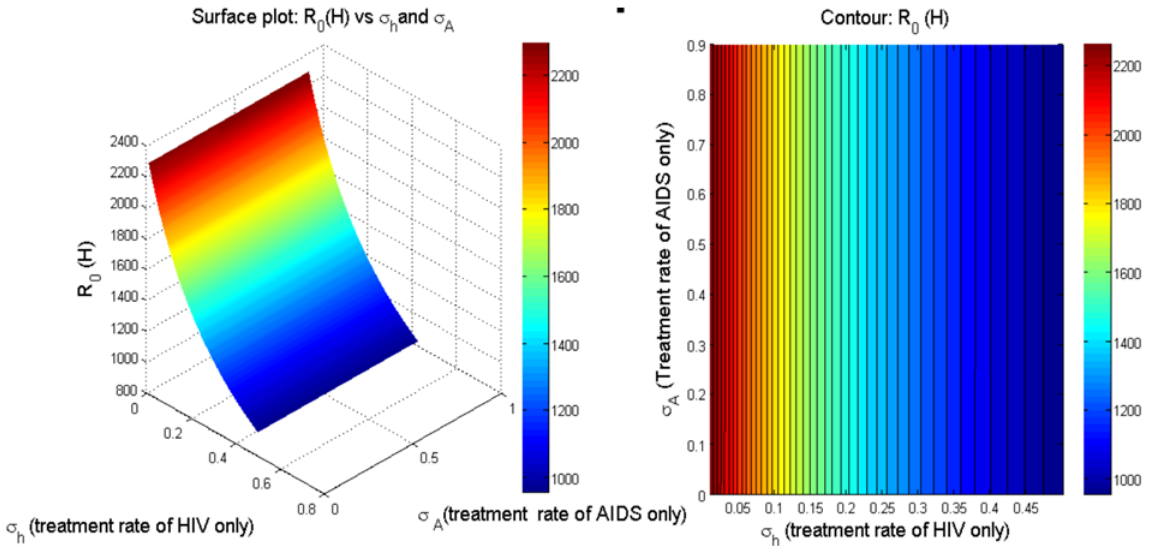

Figure 4: Contour and surface plot showing the impact of σ_h and σ_A on R_0^H

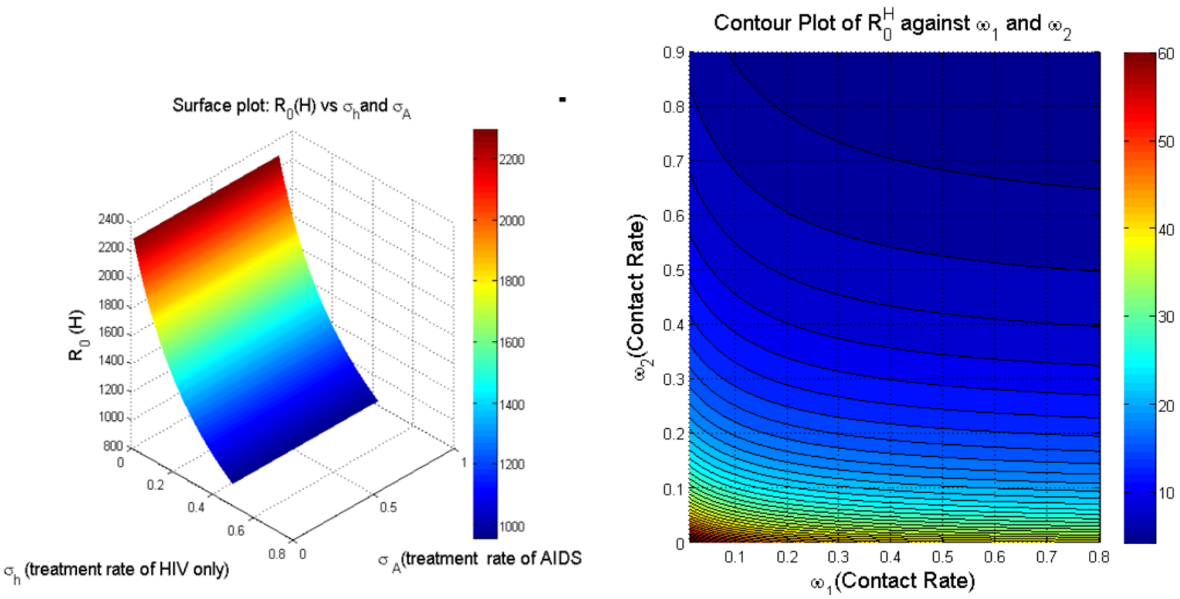

(a) Surface plot showing the impact of ω_1 and ω_2 on R_0^H

(b) Contour plot showing the impact of ω_1 and ω_2 on R_0^H

Figure 5: Contour plot of the basic reproduction number

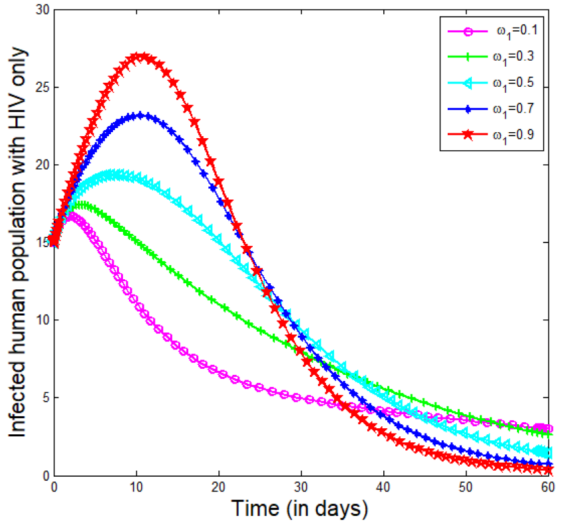

(a) Simulation of the effect of ω_1 infected individuals with HIV only

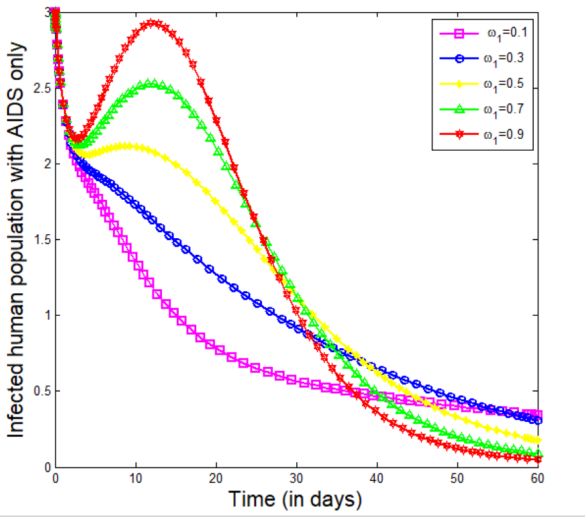

(b) Simulation of the effect of ω_1 on infected individuals with AIDS only

Figure 6: Simulation of the effect of ω_1 on infected individuals with HIV and AIDS

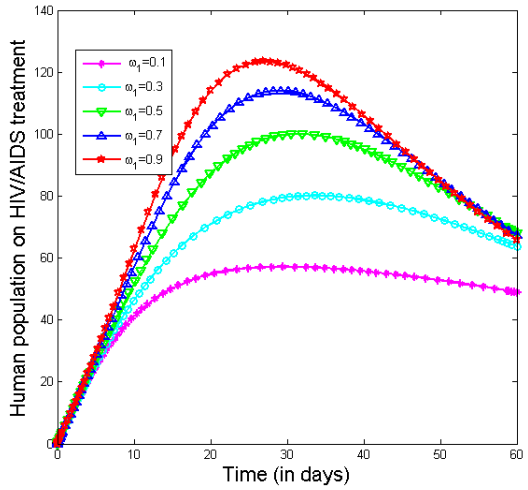

(a) Simulation of the effect of ω_1 on individuals with HIV and AIDS treatment

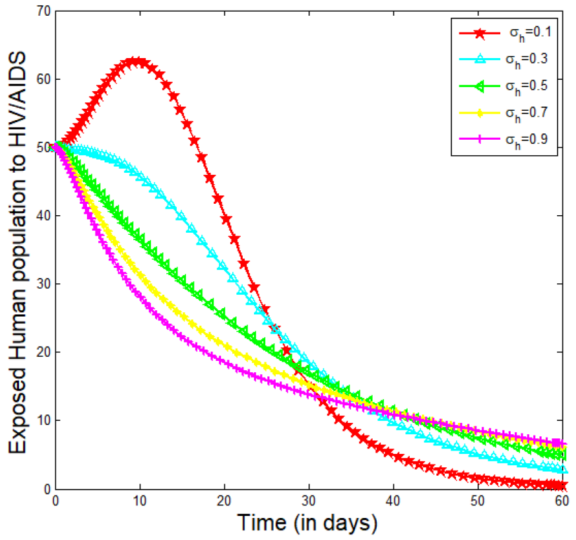

(b) Simulation of the effect of σ_h on exposed individuals to HIV and AIDS

Figure 7: Simulation of the effect of σ_h and ω_1 on on treatment and exposed individuals to HIV and AIDS

Figure 4 illustrates the combined surface and contour plots of R_0^H against HIV treatment rate σ_h and AIDS treatment rate σ_A. The surface plot shows that R_0^H decreases with increasing treatment rates of either type. Biologically, this means that better treatment in both the HIV and AIDS phases decreases the transmission of the disease and the total infection pressure in the population. The highest values of R_0^H occur when both σ_h and σ_A are low, representing sustained transmission. However, R_0^H decreases as either parameter increases, with the greatest decrease observed when both treatment rates are high. Likewise, from the contour plot, R_0^H is the highest in the region where both σ_h and σ_A are low, which means strong and sustained transmission. As σ_h or σ_A increases, R_0^H decreases progressively, and lower values are achieved when both treatment rates are high. This further confirms the importance of effective com-

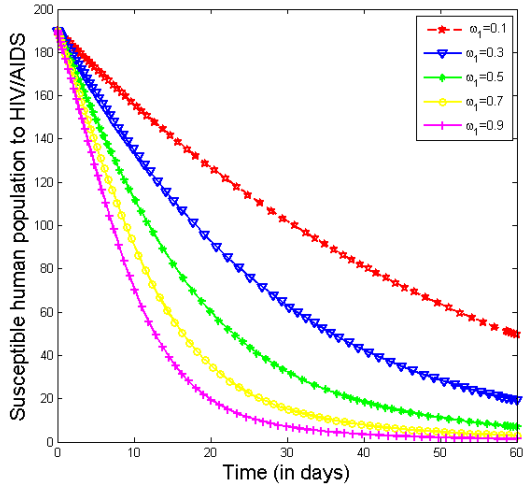

(a) Simulation of the effect of ω_1 on susceptible individuals to HIV and AIDS

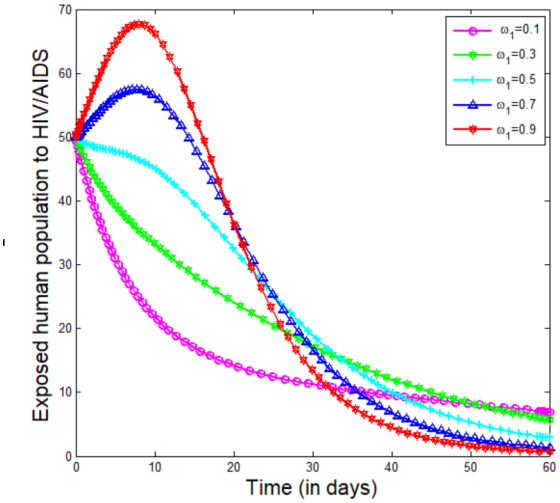

(b) Simulation of the effect of ω_1 on exposed individuals to HIV and AIDS

Figure 8: Simulation of the effect ω_1 on Susceptible and Exposed humans to HIV/AIDS

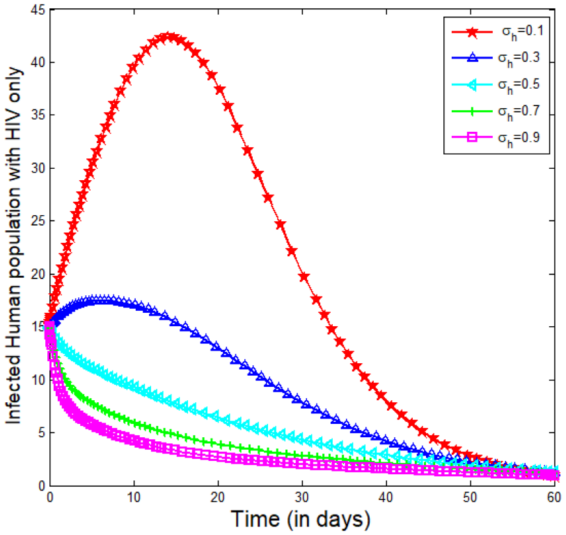

(a) Simulation of the effect of σ_h on infected individuals with HIV only

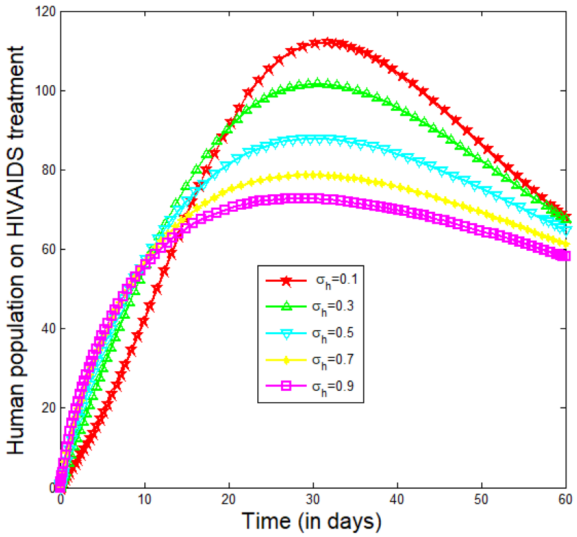

(b) Simulation of the effect of σ_h on individuals on HIV/AIDS treatment

Figure 9: Simulation of the effect of σ_h infected individuals with HIV only and individuals on HIV/AIDS treatment

bined treatment strategies at both stages of infection in reducing transmission dynamics and achieving $R_0^H < 1$ for effective control of the spread of HIV/AIDS. The surface plot of R_0^H as a function of the contact rates ω_1 and ω_2 is shown in Figure 5a.

The results indicate that R_0^H increases with increasing contact rate, i.e., the interaction of susceptible and infected individuals can enhance the transmission of HIV. The highest values are obtained when both ω_1 and ω_2 are large, while the lowest values are obtained when both are small, which may lead to $R_0^H < 1$. This suggests that the reduction of contact rates is an important factor in controlling the spread of HIV in the population. Figure 5b shows the contour plot of R_0^H versus the contact rates ω_1 and ω_2. The results show that the basic reproduction number R_0^H increases with an increase in either ω_1 or ω_2, which implies increased

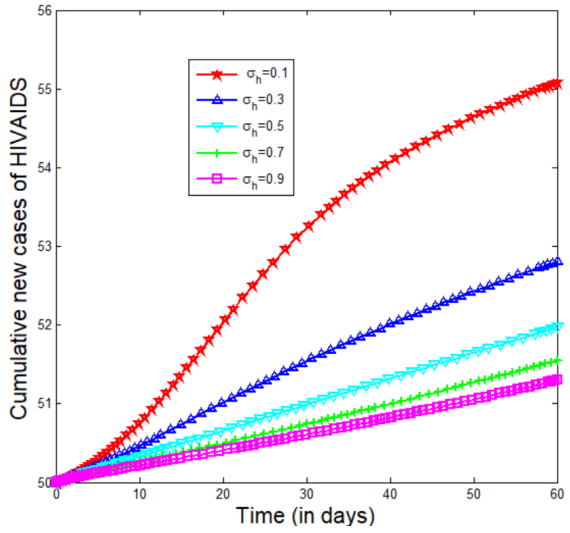

(a) Simulation of the effect of σ_h cumulative new cases of HIV/AIDS

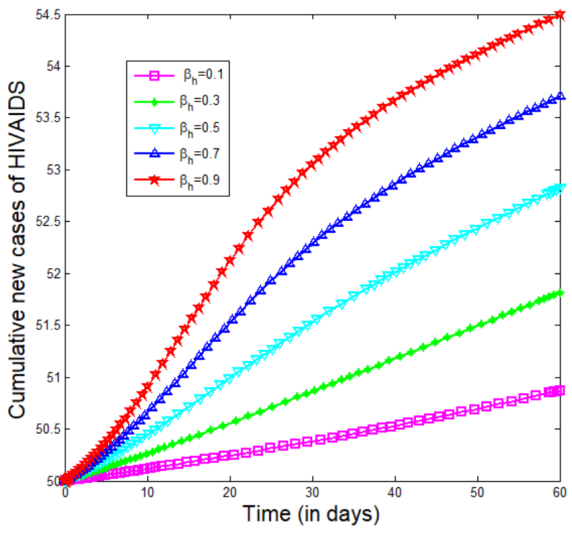

(b) Simulation of the effect of β_h cumulative new cases of HIV/AIDS

Figure 10: Simulation of the effect of σ_h and β_h on cumulative new cases of HIV/AIDS

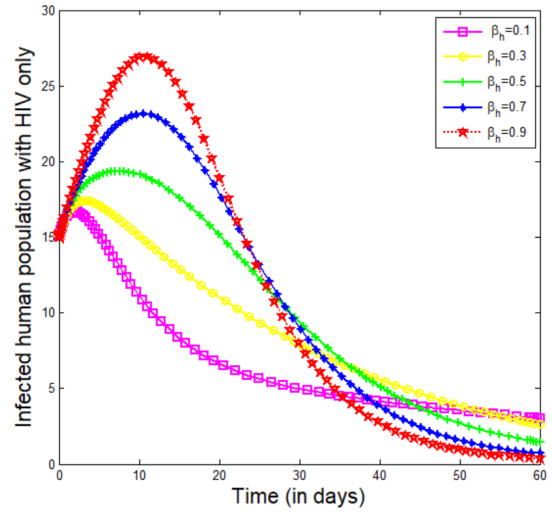

(a) Simulation of the effect of β_h on infected humans with HIV only

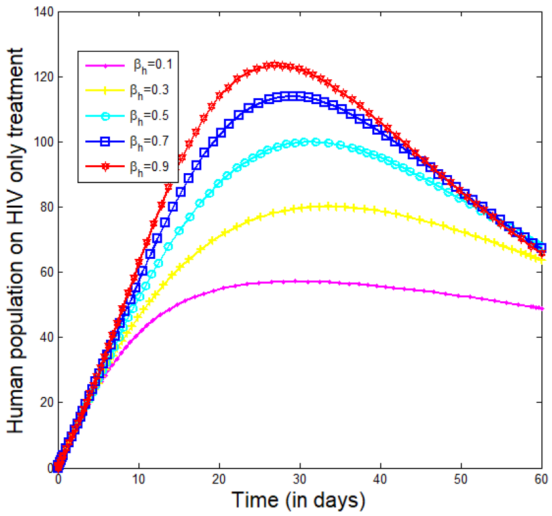

(b) Simulation of the effect of β_h on humans treatment of HIV/AIDS

Figure 11: Simulation of the effect of β_h on infected humans with HIV only and humans on treatment of HIV/AIDS

HIV transmission due to increased contact rates. The maximum values of R_0^H are obtained for large values of both ω_1 and ω_2, and the minimum values for small values of both. This suggests that reducing contact rates can significantly reduce R_0^H and help control the spread of HIV in the population. The simulation of the impact of contact rate ω_1 on the HIV-only infected population is shown in Figure 6a.

The population of HIV-positive people is seen to grow over time when the contact rate ω_1 rises. This suggests that more effective contact between susceptible and infected people increases HIV transmission within the population, leading to an increase in the number of infected people. The modeling of the impact of contact rate ω_1 on the AIDS-only affected human population is shown in Figure 6b. The population of people with AIDS is seen to

grow over time when the contact rate ω_1 rises. This suggests that increased effective contact between susceptible and infected people increases the spread of AIDS throughout the population, leading to an increase in the number of infected people. The simulation of the impact of contact rate ω_1 on the human population undergoing HIV therapy is presented in Figure 7a.

It is found that the number of people receiving HIV therapy rises over time as the contact rate ω_1 does. This implies that greater transmission rates cause more people to become infected and then need treatment, which puts additional strain on the treatment compartment. The modeling of the impact of treatment rate σ_h on the human population exposed to HIV/AIDS is displayed in Figure 7b. It is found that the exposed human population gradually declines as the treatment rate σ_h rises. This suggests that better treatment during the early stages of infection slows the progression of people from exposure to active infection, which lowers the population's overall disease burden.

The simulation of the impact of contact rate ω_1 on the vulnerable human population is presented in Figure 8a. The sensitive human population is seen to diminish over time when the contact rate ω_1 rises. This is due to the fact that increased effective contact lowers the size of the susceptible class in the population by increasing the rate at which susceptible individuals contract the disease. The simulation of the impact of contact rate ω_1 on the exposed human population is displayed in Figure 8b. It is found that the exposed human population first rises and then gradually decreases as the contact rate ω_1 increases. This indicates that higher contact rates accelerate the movement of individuals from the susceptible class into the exposed class, but sustained transmission eventually depletes the susceptible humans, leading to a reduction in the exposed population in the long run.

The simulation of the impact of treatment rate σ_h on the HIV-only infected human population is presented in Figure 9a. The population of people living with HIV is seen to decline over time when the treatment rate σ_h rises. This suggests that better treatment shortens the infectious time and viral progression, which lowers the number of people in the infected class and helps effectively limit HIV transmission in the population. The modeling of the impact of treatment rate σ_h on the human population undergoing HIV therapy is shown in Figure 9b. It is found that the population of people receiving therapy grows over time as the treatment rate σ_h rises. This suggests that increased treatment uptake and easier access to treatment push more infected persons into the treatment compartment, increasing the number of people receiving medical care. The modeling of the impact of treatment rate σ_h on the total number of new HIV/AIDS cases is presented in Figure 10a.

It is found that the cumulative number of new HIV/AIDS cases declines over time when the treatment rate σ_h rises. This suggests that when an infection is well treated, its duration and infectiousness are reduced, which limits the spread of the virus and lowers the total number of new cases in the population. The simulation of the impact of the vertical transmission rate β_h on the total number of new HIV/AIDS cases is displayed in Figure 10b. The cumulative number of new HIV/AIDS cases is seen to rise over time when the vertical transmission rate β_h rises. This suggests that increased mother-to-child transmission raises the overall incidence of new infections, which in turn raises the population's overall illness burden. The modeling of the impact of the vertical transmission rate β_h on the HIV-only infected human population is shown in Figure 11a. It is found that the number of people living with HIV increases over time as the vertical transmission rate β_h rises. This suggests that increased mother-to-child transmission sustains and raises the HIV burden in the population by bringing in a steady stream of new infected people. The simulation of the impact of vertical transmission rate β_h on the human population undergoing HIV therapy is displayed in Figure 11b. It is found that the number of people receiving HIV therapy rises over time as the vertical transmission rate β_h rises. This suggests that increased mother-to-child transmission causes more sick persons to enter the treatment class, which raises the number of people in need of assistance and medical

care.

5 Conclusions

In this study, a mathematical model was carefully developed and analyzed to study the vertical and horizontal spread of HIV/AIDS with treatment as a control measure. We calculated the basic reproduction number R_0^H of the HIV model and confirmed that the system has a forward (transcritical) bifurcation at $R_0^H = 1$.This means that the disease-free equilibrium is locally asymptotically stable if $R_0^H < 1$ and unstable if $R_0^H > 1$, and a unique stable endemic equilibrium exists when $R_0^H > 1$. Various parameters were evaluated on the effect of the R_0^H using sensitivity analysis. However, we determined that the parameters that show positive values for sensitivity indices, such as the contact rate, increase the spread and burden of HIV/AIDS in the population and so contribute to the transmission of the disease. On the other hand, the parameters that have negative sensitivity indices, which include the treatment rates σ_h and σ_A if they are negative, will also decrease the HIV/AIDS infection pressure and mitigate the transmission of HIV/AIDS. Further, numerical simulations were performed by changing the different key parameters, namely the treatment rates σ_h and σ_A, the vertical transmission rate β_h, and the contact rate ω_1.

We found that our simulations indicated that there is a significant improvement in the HIV/AIDS burden if there is an increase in treatment rates, which leads to a decrease in the number of infections and cumulative new infections in the human population, with an increase in the number of contact and vertical transmission cases worsening the spread of the disease. Overall, the results emphasize that effective combined treatment and prevention strategies are crucial for controlling HIV/AIDS transmission dynamics.

5.1 Limitations of the Study

There are some limitations to this study, which are inherent to the modelling approach adopted. First, the model is formulated in a deterministic framework, which ignores random fluctuations and stochastic effects that may influence HIV/AIDS transmission dynamics in real-world settings. Secondly, the model assumes a homogeneously mixed population, implying that all individuals have an equal probability of contact with one another, regardless of age structure, spatial distribution, social behavior, or risk heterogeneity. This assumption is commonly used in compartmental epidemic models to facilitate mathematical tractability and the analytical derivation of key epidemiological quantities such as the basic reproduction number and equilibrium states.However, in practice, contact patterns are often heterogeneous and influenced by demographic and behavioral factors, leading to non-uniform transmission dynamics. Consequently, the homogeneous mixing assumption may either overestimate or underestimate disease transmission in specific subpopulations. Despite these limitations, the model provides valuable qualitative insights into the transmission dynamics and control of HIV/AIDS and serves as a useful first approximation of the disease process. It also forms a foundation for more advanced modelling approaches, such as stochastic, network-based, or age-structured models, which may be considered in future studies.

Funding

No funding available.

Credit authorship contribution statement

J. Amos: Methodology, Writing – original draft, Formal analysis. D. Omale: Writing – review & editing, Formal analysis, W. Atokolo: Writing – review & editing, Formal analysis & editing Emmanuel Abah: Writing – review. B.A.E.Afere Writing – review, B. Bolaji: Writing – review & editing,Formal analysis. Simon Adukwu Iyaji Writing – review, Bolarinwa Bolaji: Writing – review & editing,Formal analysis.

Declaration of competing interest

No financial conflicts or personal relationships affecting the research findings of this paper exist according to the authors.

Data availability

The data used in this study are presented and referenced in table 3 of this manuscript. The source code used for simulation is available from the corresponding author on reasonable request.

References

[1] World Health Organization (WHO), HIV/AIDS, WHO, Geneva, Switzerland, 2012.

[2] Joint United Nations Programme on HIV/AIDS (UNAIDS), Overview of the Global AIDS Epidemic, Report on the Global AIDS Epidemic, ISBN: 9291734799, 2006.

[3] World Health Organization (WHO), Report on Global HIV/AIDS, WHO, Geneva, Switzerland, 2019.

[4] A. Kapila, S. Chaudhary, R.B. Sharma, H. Vashist, S.S. Sisodia, A. Gupta, A review on HIV/AIDS, Indian J. Pharm. Biol. Res. 4(3) (2016) 69–73. https://doi.org/10.30750/ijpbr.4.3.9.

[5] World Health Organization (WHO), HIV/AIDS Fact Sheet, WHO, Geneva, Switzerland, 2022. https://www.who.int/news-room/fact-sheets/detail/hiv-aids.

[6] R. Adelman, Mother-to-child HIV transmission in Africa, Policy Fact, 2001.

[7] WJ. Mushanyu, A note on the impact of late diagnosis on HIV/AIDS dynamics: A mathematical modelling approach, BMC Res. Notes 13(1) (2020) 1–8.

[8] T.K. Ayele, E.F. Doungmo Goufo, S. Mugisha, Mathematical modeling of HIV/AIDS with optimal control: A case study in Ethiopia, Results Phys. 26 (2021) 104263. https://doi.org/10.1016/j.rinp.2021.104263.

[9] C.N. Podder, O. Sharomi, A.B. Gumel, E. Strawbridge, Mathematical analysis of a model for assessing the impact of antiretroviral therapy, voluntary testing, and condom use in curtailing the spread of HIV, Differ. Equ. Dyn. Syst. 19(4) (2011) 283–302. https://doi.org/10.1007/s12591-011-0090-6.

[10] A. Nwankwo, D. Okuonghae, Mathematical analysis of the transmission dynamics of HIV–syphilis co-infection in the presence of treatment for syphilis, Bull. Math. Biol. 80 (2018) 437–492.

[11] E.J. Moore, S. Sirisubtawee, S. Koonprasert, A Caputo–Fabrizio fractional differential equation model for HIV/AIDS with treatment compartment, Adv. Differ. Equ. 2019 (2019) 200. https://doi.org/10.1186/s13662-019-2138-9.

[12] A. Omame, M. Abbas, A.-H. Abdel-Aty, Assessing the impact of SARS-CoV-2 infection on the dynamics of dengue and HIV via fractional derivatives, Chaos Solitons, Fractals.

[13] E. Jalija, J. Amos, W. Atokolo, D. Omale, U. Abah, U. Alih, P.A. Alabi, B. Bolaji, Numerical investigations on dengue fever model through singular and non-singular fractional operators, Int. J. Math. Anal. Model. 8(1) (2025) 216–242.

[14] L. Emmanuel, D. Omale, W. Atokolo, J. Amos, E. Abah, A. Ojonimi, T. Onoja, G. Acheneje, B. Bolaji, Fractional mathematical model for the dynamics of pneumonia transmission with control using fixed-point theory, GPH Int. J. Math. 8(5) (2025) 55–86. https://doi.org/10.5281/zenodo.16364036.

[15] E. Jalija, J. Amos, W. Atokolo, E. Abah, B.C. Agbata, G.O. Acheneje, B. Shyamsunder, B. Bolaji, Numerical solution of a fractional-order typhoid fever model via the generalized fractional Adams–Bashforth–Moulton approach, Netw. Model. Anal. Health Inform. Bioinform. 15 (2026) 68. https://doi.org/10.1007/s13721-026-00743-1.

[16] P.O. Odiba, G.O. Acheneje, B. Bolaji, A compartmental deterministic epidemiological model with nonlinear differential equations for analysing co-infection dynamics between COVID-19, HIV, and monkeypox diseases, Healthcare Anal. 5 (2024) 100311. https://doi.org/10.1016/j.health.2024.100311.

[17] A.A. Ojonimi, J. Amos, W. Atokolo, D. Omale, L.M. Emmanuel, E. Abah, G.O. Acheneje, B. Bolaji, Numerical solution of a fractional-order Hepatitis B model via the generalized fractional Adams–Bashforth–Moulton approach, J. Sci. Res. Rev. 2(5) (2025) 33–48. https://doi.org/10.70882/josrar.2025.v2i5.119.

[18] D. Omale, W. Atokolo, M. Akpa, Global stability and sensitivity analysis of transmission dynamics of tuberculosis and its control: A case study of Ika General Hospital Ankpa, Kogi State, Nigeria, Acad. J. Stat. Math. 6 (2020) 573–7151.

[19] D. Omale, P. Ojih, W. Atokolo, A. Omale, B. Bolaji, Mathematical model for transmission dynamics of HIV and tuberculosis co-infection in Kogi State, Nigeria, J. Math. Comput. Sci. 11(5) (2021) 5580–5613. https://doi.org/10.28919/jmcs/6080.

[20] B.I. Omede, B. Bolarinwa, P.J. Olumuyiwa, A.A. Ibrahim, F.A. Oguntolu, Mathematical analysis of the vertical and horizontal transmission dynamics of HIV and Zika virus co-infection, Franklin Open 6 (2023) 100064.

[21] J. Amos, D. Omale, W. Atokolo, E. Abah, B.I. Omede, G.O. Acheneje, B. Bolaji, Fractional mathematical model for the transmission dynamics and control of Hepatitis C, FUDMA J. Sci. 8(5) (2024) 451–463. https://doi.org/10.33003/fjs-2024-0805-2883.

[22] B. Bolaji, F. Ani, B.I. Omede, G.O. Acheneje, A. Ibrahim, A model for the control of transmission dynamics of human monkeypox disease in sub-Saharan Africa, J. Niger. Soc. Phys. Sci. 6 (2024) 1800.

[23] B. Bolaji, U.B. Odionyenma, B.I. Omede, P. Ojih, B. Abdullahi, A. Ibrahim, Modelling the transmission dynamics of the Omicron variant of COVID-19 in the densely populated city of Lagos, Nigeria, J. Niger. Soc. Phys. Sci. 5 (2023) 1055.

[24] J. Philip, D. Omale, W. Atokolo, J. Amos, G.O. Acheneje, B. Bolaji, Fractional mathematical model for the transmission dynamics and control of HIV/AIDS, FUDMA J. Sci. 8(6) (2024) 451–463. https://doi.org/10.33003/fjs-2024-0805-2883.

[25] C. Castillo-Chavez, S. Blower, P. van den Driessche, D. Kirschner, A.-A. Yakubu (Eds.), Mathematical Approaches for Emerging and Reemerging Infectious Diseases: Models, Methods, and Theory, Springer, New York, 2002, https://doi.org/10.1007/978-1-4757-3667-0.